TRANSPORTATION RESEARCH RECORD
556

Water Quality, Conduits, and Geometrics

4 reports prepared for the 54th Annual Meeting of the Transportation Research Board

TRB
TRANSPORTATION RESEARCH BOARD
NATIONAL RESEARCH COUNCIL
Washington, D. C., 1975

Transportation Research Record 556
Price $4.80
Edited for TRB by Joan B. Silberman

subject areas
22 highway design
23 highway drainage

The project that is the subject of this report was approved by the Governing Board of the National Research Council, whose members are drawn from the councils of the National Academy of Sciences, the National Academy of Engineering, and the Institute of Medicine. The members of the committee responsible for the report were chosen for their special competence and with regard for appropriate balance.

This report has been reviewed by a group other than the authors according to procedures approved by a Report Review Committee consisting of members of the National Academy of Sciences, the National Academy of Engineering, and the Institute of Medicine.

The views expressed in this report are those of the authors and do not necessarily reflect the view of the committee, the Transportation Research Board, the National Academy of Sciences, or the sponsors of the project.

LIBRARY OF CONGRESS CATALOGING IN PUBLICATION DATA

National Research Council. Transportation Research Board.
Water quality, conduits, and geometrics.

(Transportation research record; 556)

1. Road drainage—Addresses, essays, lectures. 2. Water quality—Wisconsin—Addresses, essays, lectu
3. Runoff—Addresses, essays, lectures. 4. Roads—Design—Addresses, essays, lectures. I. Title. II. Se
TE7.H5 No. 556 [TE215] 380.5'08s [625.7'34] 76-2549
ISBN 0-309-02463-3

CONTENTS

QUALITY OF URBAN FREEWAY STORM WATER

James B. Jodie, Division of Highways, Wisconsin Department of Transportation

This paper discusses the quality of storm-water runoff from urban freeways in Milwaukee, Wisconsin. The storm water from preselected areas was collected and tested to determine the concentrations of study parameters. Freeway runoff was compared with influent and effluent of the Milwaukee Sewage Treatment Plant, adopted intrastate water quality standards for Wisconsin, water from the Menominee River (which is the outfall for the freeway watersheds studied), and other national and international urban storm-water data. The results of this study indicate that the runoff from freeways in an urban area is of poor quality. Further research is needed to provide more specific data about the source of pollution so that the problem of storm-water runoff quality can be solved.

•STORM water draining from urban freeways has been criticized by some environmentalists as contributing to the pollution of adjacent ponds, streams, and lakes. As of this date, there is a lack of tangible data to either contradict or confirm statements that freeway storm water is creating an environmental problem. This project was established to determine the quality of freeway storm-water runoff in an urban area by analyzing it to determine its physical, chemical, and bacterial makeup and by comparing it with established water quality standards, sewage plant influent and effluent, and other urban storm-water runoff. The information obtained from this paper will also lay the foundation for possible future studies.

PROCEDURE FOR TEST

In July 1972, a 1-year sampling and testing program began at two storm-water outfall locations on the urban freeway system in Milwaukee County. The watersheds or drainage basins studied collected only the runoff from the freeway surface and the adjacent cut areas that drain onto the freeway. Questions asked about the watershed requirements were as follows:

1. Is the watershed typical of an urban area?
2. Has a storm sewer system been designed for the freeway segment selected?
3. Does the storm sewer system collect only water draining from the freeway pavement surface and the adjacent slopes?
4. Is there an accessible sampling location (e.g., manhole or sewer outfall)?
5. Is there a predominant land use adjacent to the freeway?

Specific features such as adjacent land developments, topography, and amount and kind of vegetative cover were noted for each watershed. This was done to locate the source of a pollutant and to associate the concentration of a parameter (pollutant indicator) with the location on the freeway. The watersheds selected were as follows:

1. The Stadium Freeway has a 48-in. (122-cm) storm sewer that has an outlet into the Menominee River at State Street. Adjacent land use is 65 percent residential, 5 percent industrial, and 30 percent parkland. The drainage area is 34 acres (13.8 hm^2) (Figure 1).

Publication of this paper sponsored by Committee on Hydrology, Hydraulics, and Water Quality.

2. The East-West Freeway has a 30-in. (76-cm) storm sewer that has an outlet into the Menominee River at the Stadium interchange. Adjacent land use is 50 percent industrial, 45 percent residential, and 5 percent parkland. The drainage area is 8 acres (3.2 hm^2) (Figure 2).

Parameters were selected that would define freeway runoff waters and that could be used as a comparison with other studies. The parameters selected were sodium chloride (NaCl), calcium chloride ($CaCl_2$), total solids, volatile total solids, suspended solids, volatile suspended solids, 5-day biochemical oxygen demand (BOD), total nitrogen (N_2), pH, total phosphorous (P), ammonia (NH_3), fecal coliforms (MFFCC), lead (Pb), dissolved oxygen (O_2), and nitrates (NO_3^-) and nitrites (NO_2^-). Other physical characteristics noted were air temperature, water temperature, form of precipitation, gasoline odor, and indications of an oil slick. The pH and dissolved oxygen concentrations were determined in the field; all other bacterial and chemical testing was conducted by the Wisconsin State Laboratory of Hygiene in Madison.

In all months, except August and October, samples were collected at least once. All samples were collected at the outfall of the freeway storm sewer system.

RESULTS OF TESTS

The results of the samples indicated the following:

1. The parameter concentrations for a sample collected in the first hour of a storm tended to be higher than those collected in the remainder of the storm.
2. The concentration of parameters tended to be very high during a snowstorm.
3. Pollutants released into the atmosphere from adjacent land developments were not detected (by observation) in the storm runoff.
4. No difference in the quality of storm water was observed between the two watersheds sampled.
5. Salt concentrations can be quite high and can have several surges of high concentrations during the winter and spring. Salt concentrations tend to taper off with the onset of summer.

A comparison of freeway runoff with adopted intrastate standards for Wisconsin (6) indicate this water is inadequate to support fish life and is unacceptable for recreational purposes. In comparison to that in the effluent from Jones Island Treatment Plant in Milwaukee (5), the concentration of phosphorous and nitrogen in the runoff is minimal (Table 1). However, the freeway runoff contains a greater concentration of total solids, suspended solids, and BOD than the effluent from the treatment plant. In accordance with a Southeastern Wisconsin Regional Planning Commission study of the Menominee River in April 1973, the runoff from both the river and the freeway is of poor quality. Comparable international studies from local streets show that urban runoff is characterized by a high fecal coliform and phosphate concentration; however, freeway runoff tends to contain high concentrations of total solids and chlorides [Table 2 (1, 9)].

Storm-water runoff from freeways contains concentrations of contaminants that make this poor-quality water. This runoff is a possible detriment to the environment. Therefore, more attention must be directed to the effect of all freeway runoff on the ecological system of an urban area. This awareness is further emphasized by anticipated increases in population and movements toward urban areas. As a result, the dependency on the automobile for employment, recreation, and industrial purposes will tend to increase. This factor, coupled with the increasing need for available water resources, places great responsibility on planning agencies to manipulate or modify the character of water, such as freeway runoff, so that it can become readily available for many beneficial uses.

Figure 1. Stadium Freeway watershed.

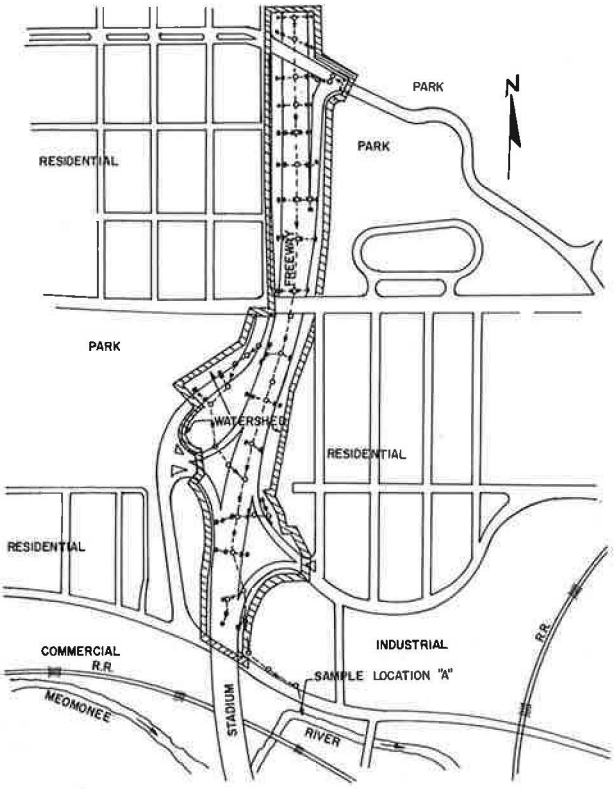

Figure 2. East-West Freeway watershed.

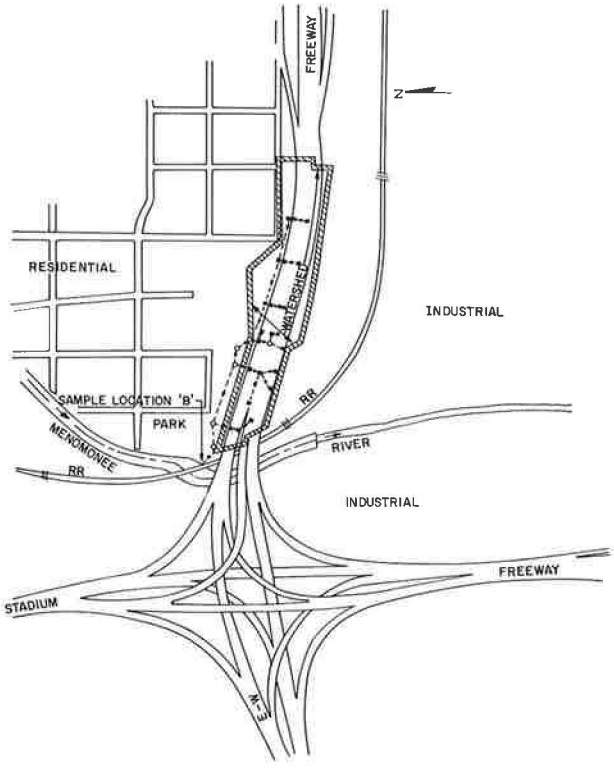

Table 1. Parameter values for Milwaukee urban freeway storm water.

Parameter	Stadium Freeway		East-West Freeway		Milwaukee Sewerage Commission (1970)			
					Yearly Avg of Screened Effluent	Plant Effluent		Menominee River
	Avg	Range	Avg	Range		West	East	
BOD	17	1.80 to 45.0	30	8.60 to 90.0	209	12.5	16.3	3.7
Total solids	5,188	244 to 26,650	7,380	156 to 54,120	939	724	759	–
Volatile total solids	393	55 to 1,050	244	54 to 570	–	–	–	–
Suspended solids	235	0 to 1,230	192	19 to 785	207	18.5	23	–
Volatile suspended solids	47	0 to 185	38	5 to 125	–	–	–	–
Cl^- as NaCl	2,606	30 to 26,000	4,128	8 to 35,000	–	–	–	98
Ca^{++} as $CaCl_2$	142	40 to 250	189	36 to 300	–	–	–	–
Total N_2	1.43	0.29 to 3.40	1.77	0.56 to 3.70	28.30	10.90	8.60	0.75
NH_3	0.49	0.05 to 1.10	0.72	0.05 to 1.40	–	–	–	0.36
Total P	0.20	0.002 to 1.06	0.21	0.02 to 0.64	8.20	1.40	0.70	0.30
Dissolved O_2	11.0	9.2 to 12.2	10.3	7.2 to 11.8	–	–	–	11.1
pH	7.7	6.3 to 9.0	7.9	7.2 to 9.3	–	–	–	8.0
Water temperature, deg C	9.3	1 to 23	9	1 to 21	–	–	–	5.8
NO_3^- and NO_2^-	1.08	0.15 to 2.00	1.51	0.24 to 2.60	–	–	–	1.70
MFFCC*	2,750	100 to 6,200	1,600	1,300 to 1,900	–	–	–	1,210
Pb	0.90	0.71 to 1.10	0.84	0.56 to 1.00	–	–	–	–

Note: With the exception of pH, water temperature, and MFFCC, all concentrations are expressed as mg/liter. MFFCC values are expressed as membrane filter fecal coliform count/100 ml.

*Total coliforms = 5 x MFFCC = 25,000 (3).

Table 2. Storm-water quality from urban drainage basin in Milwaukee.

Location	Type of Runoff	Measurement	BOD (mg/liter)	COD[a] (mg/liter)	Total Solids (mg/liter)	Volatile Solids (mg/liter)	Suspended Solids (mg/liter)	Total Phosphate (mg/liter)	Fecal Coliforms/ 100 ml[b]	Cl^- as NaCl (mg/liter)
Durham, N.C.	Urban storm water	Mean	14.5	179	2,730	298	–	0.58	30,000	12.6
		Range	2 to 232	40 to 600	274 to 13,800	20 to 1,110	–	0.15 to 2.50	7,000 to 86,000[c]	3.0 to 390
Cincinnati, Ohio	Urban storm water	Mean	17	111	–	–	227	1.1	–	19.8
		Range	1 to 173	20 to 610	–	–	5 to 1,200	0.02 to 7.3	500 to 76,000	5.0 to 705
Cincinnati, Ohio	Rainfall	Mean	–	16	–	–	12	0.24	–	–
Coshocton, Ohio	Rural storm water	Mean	7	79	–	–	313	1.7	–	–
		Range	0.5 to 23	30 to 159	–	–	5 to 2,074	0.25 to 3.3	2 to 56,000	–
Coshocton, Ohio	Rainfall	Mean	–	9.0	–	–	11.7	0.08	–	–
Detroit, Mich. (1949)	Urban storm water	Range	96 to 234	–	310 to 914	–	–	–	–	–
Seattle, Wash.	Freeway storm water	Range	9 to 198	103 to 1,617	–	–	11 to 1,494	0.14 to 0.51	–	–
Stockholm, Sweden	Urban storm water	Median	17	188	300	90	–	–	4,000	–
		Maximum	80	3,100	3,000	580	–	–	200,000	–
Pretoria, South Africa										
Residential, park, and school			30	29	–	–	–	–	240,000	–
Business and flat area			34	28	–	–	–	–	230,000	–
Oxney, England		Maximum	100	–	–	–	2,045	–	–	–
Leningrad, USSR			36	–	–	–	14,541	–	–	–
Moscow, USSR		Range	18 to 285	–	–	–	100 to 3,500	–	–	–
Milwaukee, Wisc.	Urban freeway storm water	Avg	24	–	6,202	324	215	0.20[d]	2,367	3,298
		Range	1.8 to 90.0	–	156 to 54,120	54 to 1,050	0 to 1,230	0.002 to 1.06	100 to 6,200	8 to 35,000

[a]Chemical oxygen demand. [b]Total coliforms (MPN/100 ml) = 25,000 to 930,000. [c]Range of means for 17 storm series. [d]Total phosphorus.

SUGGESTION FOR FUTURE RESEARCH

Except for the study made in Seattle, Washington (2), the runoff data pertinent to urban freeways is nonexistent. Therefore, the information obtained from this report would, in effect, lay the foundation for future studies of a similar nature.

In general, the methods used in this project provided valid information for a determination of the quality of freeway storm-water runoff. However, a program of continued research is vital to further define this storm water, to locate the sources of pollution, and to determine the full impact of this water on the environment. The objectives of future research should be to answer the following:

1. Is it necessary that this water be treated, or should its environmental impact be diminished by some other means?
2. Is the volume of storm water insignificant (compared with the volume of urban storm-water runoff from all of Milwaukee)?
3. Under what conditions (volume, concentration, and type of pollutant) would treatment of this runoff be necessary?
4. What are the economics of alternate measures of dealing with this water?

If additional research indicates that pollution by freeway runoff is significant, then this research should include solutions to the problem, such as treatment at the outfall, impounding reservoirs, or cross connections to combined sewers. To satisfy public demands and federal requirements, the information should then be placed in environmental impact statements listing the existing and projected water quality conditions. Then, either the insignificance of storm water can be verified, or solutions to the problem of storm-water disposal can be included as part of a project cost. However, the solution of freeway runoff problems will only be made possible by continued research.

REFERENCES

1. E. H. Bryan. Quality of Stormwater Drainage From Urban Land. Proc., 7th American Water Resources Conference, Washington, D.C., 1971.
2. R. D. Dalseg and G. D. Farris. The Quality of Rainfall Runoff From Interstate 5 at Seattle. Municipality of Metropolitan Seattle, 1970.
3. Selected Biological, Chemical and Physical Parameters—Lower Menominee River. NSF-SOS Institute, Marquette Univ., 1972.
4. R. E. Hanes, L. W. Zelazny, and R. E. Blaser. Effects of Deicing Salts on Water Quality and Biota. NCHRP Rept. 91, 1970.
5. Milwaukee Sewerage Commission. Phosphorous Removal With Pickle Liquor in an Activated Sludge Plant. Prepared for Environmental Protection Agency, Project 11010 FLQ, March 1971.
6. Water Quality and Flow in Streams in Southeastern Wisconsin. Southeastern Wisconsin Regional Planning Commission. Technical Rept. 4, Nov. 1966.
7. Menominee River Watershed Planning Program Prospectus. Southeastern Wisconsin Regional Planning Commission, Nov. 1969.
8. Standard Methods for the Examination of Water and Waste-Water. American Public Health Association, American Water Works Association, and Water Pollution Control Federation, 13th Ed., 1972.
9. S. R. Weibel, R. B. Weidner, A. G. Christianson, and R. J. Anderson. Characterization, Treatment, and Disposal of Urban Stormwater. Proc., 3rd International Conference on Water Pollution Research, Water Pollution Control Federation, Washington, D.C., 1966.

COMPOSITE CONDUIT CONSTRUCTION FOR LOWER COST INSTALLATIONS AND IMPROVED PERFORMANCE

Thomas K. Breitfuss, Hydro Conduit Corporation

Substantial reductions in material costs of conduits may be obtained by partially or fully surrounding specially designed thin-shelled core units with structurally bonded concrete or with a combination of concrete and soil-cement. Analyses are made of composite concrete conduits with side support varying from undisturbed trenches through recompacted soil to those with no lateral support. Analyses are made of controlling moments, shears, and thrusts for various angles of encasement at the bottom and sides or for encasement fully surrounding the core units. From these values, comparisons are made of allowable loads on unreinforced concrete composite conduits and of relative amounts of tensile reinforcement required in reinforced conduits. Tests are described in which performance and installations of conventional pipe sections are compared with those of composite sections under similar loads to verify previously described analyses.

•THERE is a continuing search for ways to improve conduits and to reduce costs simultaneously, if possible. Shortages of construction materials and of construction funds have accelerated this search.

This paper will describe new soil-structure systems as a means of obtaining both improved costs and improved performance of pipelines.

The concepts involve specially shaped and designed preformed core units used in the field with structural stiffening and supporting materials bonded to selected areas around the core's periphery. This assembly is installed in specially designed trenches or embankments, as shown in Figure 1.

One can obtain more than the sum of the advantages of precast and cast-in-place pipeline construction by combining advantageous features of each. Design analyses showed substantial savings in reinforcing steel and concrete. Construction cost analyses showed additional savings and a superior, more reliable conduit.

The preformed core can be thin and light in weight or thin only where thickness is not required. The composite conduit would then have special tensile and compressive characteristics in essential areas. Cores could incorporate flexible joints, preformed joints, corrosion-resistant linings, pressure linings, velocity reducers, or numerous other features. Thin, light cores made under controlled conditions can be manufactured, transported, and assembled at much lower cost than today's conventional conduits. A machine (U.S. Pat. 3,830,606), which doubles as a trench shield, can be used to install and surround core units in narrow or wide trenches to further reduce installation costs.

The medium or mediums between the core and the earth itself are essential components of the system. The medium might be conventional soil backfill, select dense sand, soil-cement, structural concrete, a spongy cushion, or combinations of these in selected areas. This paper deals primarily with theories and tests of round rigid concrete type conduits, although many adaptations are obtainable for other types of conduits

Publication of this paper sponsored by Committee on Subsurface Structures Design.

that depend on lateral support for installed strength. Primary analyses concern rigid structural in situ mediums structurally bonded to at least portions of the core and comparative tests with other mediums. Besides the structural advantages, a concrete medium obviates the need for select bedding. Grade maintenance and core support are interdependent, and minimum trench widths reduce loads and avoid wasting concrete backfill. Thus, the concept is somewhat self-governing in ensuring that construction will comply with design and thereby avoid major disputes about compliance with trench width, bedding, and backfilling specifications and high bedding-termination stresses (1).

This paper focuses on installations in narrow trenches formed in undisturbed supportive soil or in dense backfill. These trenches are shaped to the general configuration of the lower periphery of the core.

The advantages of a narrow trench are manifold (2, 3). Less excavation backfill and restoration are required as is less right-of-way. Earth loads are smaller because of the narrow trench.

This paper then deals primarily with the structural cost-related advantages of using thin, preformed, round concrete core units with a rigid surrounding medium bonded to selected areas of the core to act structurally with it in a narrow trench.

ECONOMIC ANALYSIS OF STRUCTURES

Hydro Conduit Corporation undertook economic analyses of composite construction a few years ago. It appeared that savings of up to 30 percent of the then current installed costs of concrete pipe conduits could be realized. Obviously savings varied as conduit diameters and the evaluated depths and types of installations varied. Rigorous structural analyses and field testing appeared to be justified and were undertaken.

Structural composite action depends on shear transfer between bonded elements of nonlaminated and laminated beams (bottom and top respectively, Figure 2). This transfer differentiates composite conduits from encased conduits. Effective shear transfer increases the load-carrying ability by a factor of 4 for the same deflection or by 2 for the same unit stress in Figure 2. Before testing full-scale pipe, extensive tests of beams were conducted in 1971 to determine the reliability of various bonding agents in transferring shear between new and hardened concrete. Results (4) indicated, as expected, that mechanical keys were the most effective but that various lesser degrees of tensile strength and shear transfer could be developed between roughened surfaces or at the interface by using certain chemical agents or chemical agents and mechanical keys.

These beams were tested by applying concentrated loads at the midpoint. Field loading on conduits is actually imposed more uniformly as shown by classical pressure distributions in Figure 3. So that reliable bond and shear values can be established, the criterion of bond or means of shear transfer and related moment resistance should be further verified by tests of composite beams of design thickness that are loaded uniformly to produce the desired moments. Thus, one can determine the effectiveness of various bonding means such as portland cement, chlorinated rubber, epoxies, spiked or roughened surfaces, and keyed surfaces.

COMPARATIVE ANALYSES

Several configurations of composite construction can be compared analytically with one another and with conventional construction for degrees of efficiency. Eight types of conduits with 60-in. (1524-mm) internal diameters are shown in Figure 4; a conventional 60-in. (1524-mm) conduit is shown in Figure 4a; composite conduits are shown in Figure 4b, c, d, e, g, and h; and a thin-walled conduit with a soil-cement encasement is shown in Figure 4f. At the left of each figure are moments at the top, sides, and bottom. At the right are values of t^2W/M [in inches (1 in. = 25.4 mm)], which is proportional to the maximum load that can be supported safely by an unreinforced conduit, and M/Wd, a nondimensional measurement, which is directly related to the tensile

Figure 1. Composite core with top and bottom bonded encasement in a narrow trench.

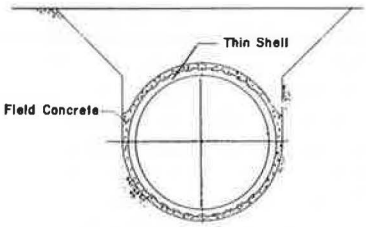

Figure 2. Nonlaminated and laminated beams.

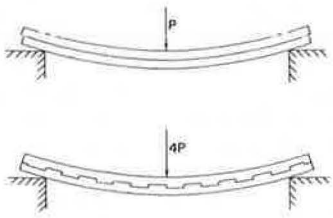

Figure 3. Assumed distribution of earth loads and support on buried composite conduit.

Figure 4. Eight types of conduits with 60-in. (1524-mm) internal diameters.

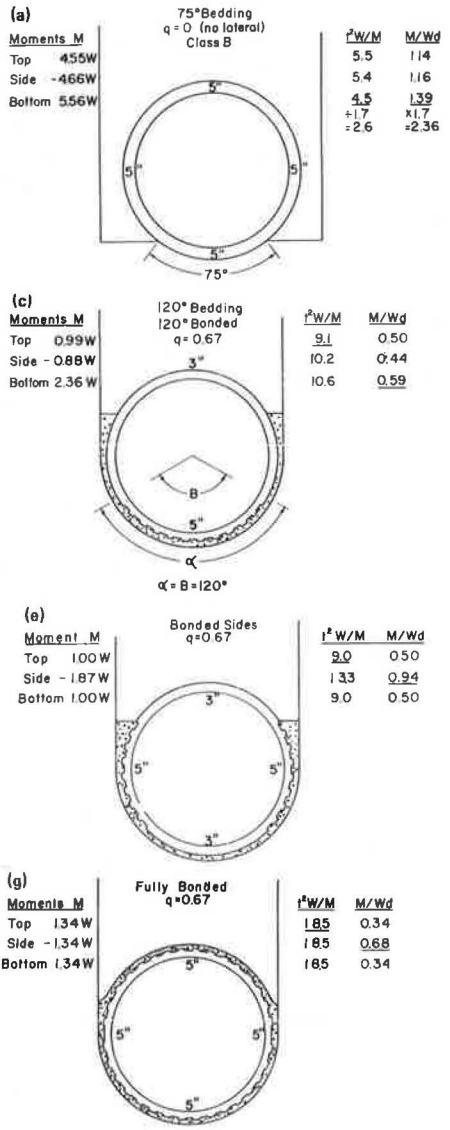

steel required in a reinforced conduit, where t is the wall thickness of either the core or the bonded composite section, M [in pound-force-inch (1 lbf-in. = 0.1130 N·m)] is the moment at the section being analyzed, W is the load on the conduit, and d is the effective moment resisting lever arm from the compressive face to the tensile steel in reinforced sections. For unreinforced conduits controlled by flexural strength, the extreme fiber stress f_t is equal to the moment M at the section times c, half the wall thickness, divided by I, the moment of inertia of the section. Rearranged,

$$M = f_t I/C = (f_t bd^3/12)/(d/2) = f_t 2d^2 \quad (1)$$

If f_t is set equal to an allowable value of $5\sqrt{f_c'}$, where f_c' is the 28-day compressive strength at the extreme fiber and K is a coefficient which, when multiplied by W, computes the moment at that section (M = KW), then the maximum load is

$$W = (2)(5)\sqrt{f_c'}\, t^2/K \quad (2)$$

Thus, for a given cross section t^2/K, the values of Wt^2/M are directly proportional to W. The lowest value will determine W_{max} for a conduit.

Similarly, for reinforced conduits

$$A_s = M/f_s jd = (KW/f_s jd)\, K/d \quad (3)$$

Therefore, M/Wd is proportional to the tensile steel required at reinforced sections, and the highest value controls the tensile steel requirements. (Probable controlling values are underlined in Figure 4.)

Moments, thrusts, and shear are based on arch theory analysis modified to reflect certain differences between pipe and arches (5). Earth loads W are assumed to act over the top 180 deg of the conduit. Bedding in Figure 4b, c, d, e, f, g, and h is assumed to be 180 deg, and the ratio of passive lateral support to vertical load q is assumed to be 0.67 in the undisturbed firm soil trenches.

Originally, side support for composite conduits was assumed to be 33 percent of the vertical load. A subsequent study was conducted to determine more accurate values of q for undisturbed trench sides with soil-cement backfill, dense sand backfill, and concrete encasement. From known loads on the pipe tested in Phoenix and reported later in this paper, Smith (6) determined analytically what lateral support would be required to restrict deflection of the pipe sections to the measured values. These were determined to be 0.33 for dense sand in a trench 2 ft (0.6 m) wider than the pipe, 0.60 for soil-cement, or 0.67 for concrete as side backfill in a narrow trench. The coefficient of lateral to vertical load for embankment culverts is not known but would logically lie between 0 and 0.6. The two-band criteria (established by California Department of Transportation) for pipe culverts specify values between 0.30 and 1.0. A value of 0.33 would seem to be conservative.

The composite designs used are variations of a 3-in.-thick (76-mm) core section or a core of variable wall thickness with 1 or 2 in. (25 to 51 mm) of exterior concrete bonded to selected areas. Bonding is indicated by the staggered interface between the core and envelope. Figure 5 (5) shows the general arrangement of segments in a composite section somewhat similar to Figure 7b, in which the top 240 deg are thin and the lower 120 deg are thick and there is a transition segment between.

Earth load W for trench conduit designs may be determined from Marston-Spangler formulas. Coefficients for moment, thrust, and shear in terms of W for unit diameters were computed at 15-deg increments from top to bottom for 180-deg bedding and various lateral support values.

Analyses should first be made of flexural strength of nonreinforced conduits for maximum economy. Comparisons in this paper are based on allowable flexural stress in the extreme fibers of $5\sqrt{f_c'}$. Obviously, no steel or steel for handling only is required in these designs. When imposed loads induce higher stresses than are allowed in the unreinforced composite section, the design control shifts to reinforced concepts.

Water in the conduit and pipe-weight effects have been neglected in these comparisons. Moments due to pipe weight may reasonably be disregarded because the nature of installation tends to hydrostatically load the pipe externally and, thereby, relieve such stresses.

Open-Topped Conduits

In Figure 4a, the lowest value of t^2W/M, 4.5, governs the allowable load W. If f_c' = 5,500 psi (37.9 MPa) and there is no reinforcement,

$$W_{max} = 2\ (5)\ \sqrt{5{,}500}\ (4.5) = 3{,}337\ \text{lb/ft}\ (48\ 690\ \text{N/m}) \tag{4}$$

With 120-lb/ft^3 (1920-kg/m^3) material in a 9-ft-wide (2.7-m) trench, the fill would be less than 3 ft (0.9 m), and the effective value of t^2W/M would be 2.6. This figure is used for later comparisons (the 1.7 divisor represents W_{wide}/W_{narrow} for trenches).

Considering a reinforced section, W for a 9-ft-wide (2.7-m) trench conduit is about 1.7 times W for a 6-ft-wide (1.8-m) composite conduit. The resisting moment arm d is about 4 in a 5-in. (127-mm) wall. Therefore, the critical value of M/Wd is 5.56 at the bottom times 1.7/4 = 2.36, the highest value of M/Wd. These numbers will be used for comparisons to determine relative steel areas required in composite conduits.

Figure 4b is basically a 3-in. (76-mm) core with idealized shear transfer notches and bonded concrete somehow encasing the lower 210 deg. The lowest value of t^2W/M, 10.7, governs the design used to compute the maximum safe load on the conduit. (Note this is 4 times the value in Figure 4a. Figure 4b also takes into account the narrow trench.)

Assuming f_c' = 5,500 psi (37.9 MPa) and f_t = 371 psi (2.56 MPa), W = (2)(371)(10.7) = 7,935 lb/ft (115 770 N/m) [versus 3,337 lb/ft (48 690 N/m) in Figure 4a]. If the 120-lb/ft^3 (1920-kg/m^3) material is used for backfill, the allowable height of fill is 16 ft (4.9 m) in a 6-ft-wide (1.8-m) trench. It is evident not only that the composite section can take a much greater load but also that the allowable height of fill is increased dramatically with the narrower trench.

For reinforced core units of Figure 4b with a steel cover of 1 in. (25 mm), the maximum value of M/Wd, 0.75, would control the steel design of an elliptically placed cage because the effective value of d is only 2 in. (51 mm). However, 0.75 is still only 32 percent of 2.36 for the class B installation of Figure 4a.

It may not be possible to obtain composite action at the sides at a reasonable cost. The direction of forces at the top and bottom enhances composite performance at the notched interface, but these forces are reversed at the sides. Therefore, in Figure 4c only the lowest 120 deg are bonded, and the design is balanced for nonreinforced sections.

The allowable load on nonreinforced sections in Figure 4c is 15 percent less than that of the fully bonded conduit in Figure 4b, but the reinforcement requirements are theoretically reduced another 21 percent, and the core is probably less costly to manufacture. Inadvertently decreasing the thickness of the composite section to 4½ in. (114.3 mm) at the bottom makes 8.5 the controlling value of t^2W/M at the top, a reduction of 7 percent in W_{max}. However, the controlling value of the reinforced section becomes 0.61, which is almost unchanged.

The composite action at the bottom is beneficial for the reinforced section in Figure 4c, in which an effective d-value is 4 in. (102 mm). However, d at the sides is still only 2 in. (51 mm), and this results in the controlling value of 0.59. This can be im-

proved further if the side walls are thickened or if steel is placed in the envelope at the sides. The use of a thickened section is shown in Figure 4d. This thickening results in a balanced reduced design in which 0.47 becomes the controlling value that is only 20 percent of 2.36 required in the trench conduit in Figure 4a. In addition, the total concrete in the core and envelope is only 75 percent of that in the ASTM A-wall pipe (U.S. Pat. 3,812,884). Thickened sides and notched tops or bottoms are principal novel features of this construction and may well be the most economical construction for conduits over 6 ft (1.8 m) in diameter.

Figure 4e shows the effect if bond and shear transfer are obtained at the sides but are not obtained at the bottom. Excessive stiffness and moments are redistributed such that, at side portions, steel requirements increase by 60 percent over those in Figure 4c.

Soil-Cement Medium

A thin-walled pipe made of soil-cement or unbonded concrete is shown in Figure 4f. Encasement provides 180-deg support but no provisions for bond. Moments are equal as indicated, and t^2W/M is 6.9, which is 25 percent less than in Figure 4c. Inasmuch as W is proportional to the square of t for unreinforced, uncracked sections, uniform thin sections are less desirable. In comparison, the thickened bottom of the composite pipe in Figure 4c attracts moment from the other quadrants and makes them all more effective.

M/Wd in Figure 4f is 0.66, which is 12 percent less efficient than the 120-deg bonded unit of Figure 4c and 40 percent less efficient than the unbalanced unit in Figure 4d. Without a bond, there is no structural benefit given to the core by soil-cement. The principal benefit is in construction when a reduced trench width and improved lateral support are used. Soil-cement bedding may not perform as predicted unless foundation conditions are known. For example, line bearing may occur on a rigid foundation if the core is placed directly on the subbase. Conversely, soil-cement will not afford improved rigidity on softer foundations.

One might suggest increasing the soil-cement bedded core uniformly to 4 in. (102 mm) in thickness, but this starts the cycle again because there would be similar structural benefits with 1-in. (25-mm) thicker walls in each previously analyzed design. Thus an ideal balance is desired among costs of cores, envelopes, reinforcing, and installation after moments and shear have been considered in the installed condition. In summary, for open-topped sections, the best combination appears to be a 120-deg bottom bonded with soil-cement at the sides to provide 180-deg support. Thickened sides would gain considerably more for reinforced larger diameters.

Full Encasement

Figure 4g shows 360-deg encasement that is bonded and rigid and that results in excellent flexural values and in low steel requirements for the top and bottom. Full encasement also allows formation of joints and bends in forming the conduit and preformed flexible joints. If full advantage is taken of balanced moments for reinforced sections, the sidewall thickness has to be increased to at least 5 in. (127 mm) to make d equal 4 in. (102 mm). An effective value of 4 for d at the sides might also be obtained by reinforcing the envelope, potentially reducing M/Wd to 0.34. This would be practical for large-diameter conduits.

If a bond cannot be readily obtained at the sides, the design of Figure 4h would apply in which only the top and bottom are bonded. With a 3-in. (76-mm) wall and a 2-in. (51-mm) envelope, the values are as shown in Figure 4h. This is a reasonably balanced design that has low steel areas.

Other Shapes

Consideration might also be given to greatly exaggerated differing wall thicknesses. Consider a pipe with a 60-in. (1524-mm) internal diameter and with top and bottom walls as shown in Figure 6. Figure 6a shows a pipe with uniform wall thickness; Figure 6b a pipe of unbalanced design.

Controlling moments and values of t^2W/M and M/Wd for 180-deg load, 180-deg bedding, and 0.67 lateral support based on Figure 6 are given in Table 1.

The values in Table 1 indicate an advantage of about 0.30 percent in reduced reinforcement, and a small increase in flexural strength will be obtained by unbalancing wall thicknesses.

Cases should also be considered in which lateral support will be removed because of subsequent adjacent excavations. Comparisons similar to those in Figure 4a, c, f, and h are shown in Figure 7a, b, c, and d respectively. In Figure 7, moment, shear, and thrust values have been computed assuming a 180-deg load but only 120-deg bedding and no lateral support.

There are many other possible variations of core and encasement construction. Off-center core units could be made on existing machines; the thick side could be down for light fills, and the soil-cement backfill could be reversed with a composite bottom section for greater loading.

ALLOWABLE FILLS

For economy, the same equipment should be used to make plain or reinforced core units. Thus, units of a specific diameter may be designed both for closed- and open-topped construction. Several factors beyond the scope of this paper such as normal fill heights, joint types, and joint spacings also determine the basic core unit to be used.

The following example shows use of the concepts in design. Consider a conduit with a 60-in. (1524-mm) internal diameter and a 3-in. (76-mm) core used in a trench with 120-lb/ft^3 (1920-kg/m^3) saturated top soil as backfill.

In an open-topped composite conduit, and in Figure 4c, if $f_c' = 6{,}000$ psi (41.4 MPa), the maximum W would be

$$W = 2\,(5)\,\sqrt{6{,}000}\,(9.1)/1.2 = 5{,}874 \text{ lb/ft } (85\,700 \text{ N/m}) \tag{5}$$

This represents 13 ft (4 m) of cover. No structural reinforcement would be required because the section is designed not to crack.

If reinforced pipe is specified and a design stress of 40,000 psi (275.8 MPa) is used,

$$A_s = M/0.875\,(40{,}000)\,d = (2.36)\,(1.2)\,(5{,}874)/35{,}000\,(5 - 1) = 0.12 \text{ in.}^2\text{/ft } (2.6 \text{ cm}^2\text{/m}) \tag{6}$$

For class B bedded pipe, in an $8\frac{1}{2}$-ft (2.6-m) trench,

$$W = 1.2\,(9{,}899) = 11{,}879 \text{ lb/ft } (173\,000 \text{ N/m}) \tag{7}$$

For the test pipe,

$$\text{load} = 142{,}548 \text{ lb/ft}/60\text{-in.-diameter}/1.9 \text{ load factor} = 1{,}250\,D \quad (173\,000 \text{ N/m}/1524 \text{ mm}/1.9 = 59.8\,D_{s1}) \tag{8}$$

Figure 5. Finite element model of conduit in which top 240 deg are thin and bottom 120 deg are thick.

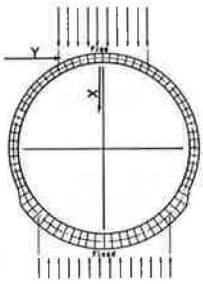

Figure 6. Uniform-wall pipe (a) compared with pipe of unbalanced design of similar total weight (b).

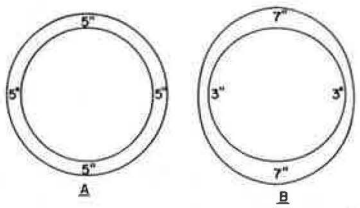

Table 1. Controlling moments and values of t^2 W/M and M/Wd for 180-deg load, 180-deg bedding, and 0.67 lateral support based on Figure 6.

	Controlling Moment		t^2W/M		M/Wd	
Item	Uniform Thickness	Unbalanced Design	Uniform Thickness	Unbalanced Design	Uniform Thickness	Unbalanced Design
Top	1.35W	1.49	18.5	33.0	0.34	0.25
Sides	-1.35W	-0.44	18.5	20.0	0.34	0.22
Bottom	1.35W	1.49	18.5	33.0	0.34	0.25

Note: Underscored numbers are probable controlling values.

Figure 7. Four types of construction without lateral support.

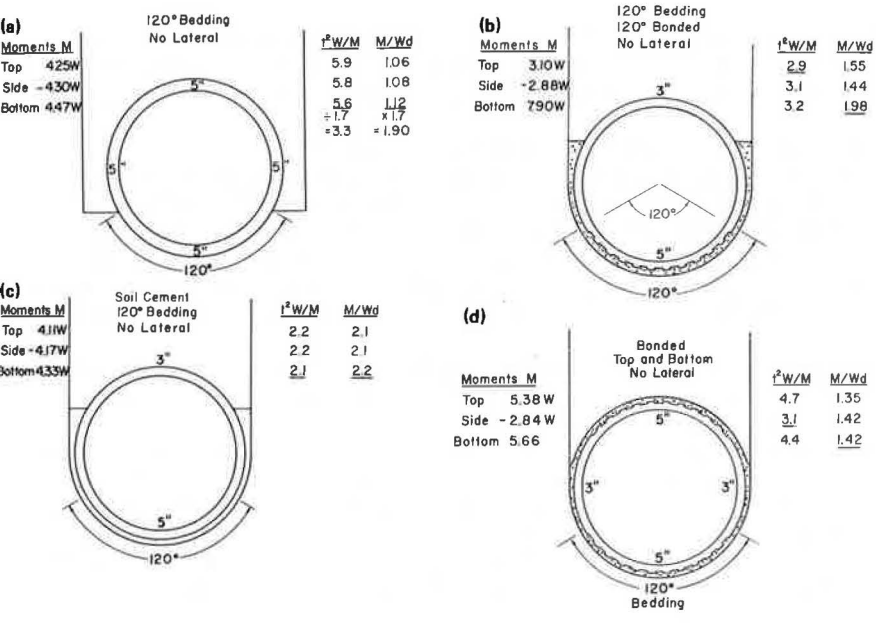

A_s is about 0.47 in.^{2}/ft (10 cm^2/m). Checking by moments gives

$$A_s = (5.56)\ (11{,}879)/(0.875)\ 40{,}000\ (4) = 0.47 \text{ in.}^2\text{/ft } (10 \text{ cm}^2\text{/m})$$

Savings are 79 percent in steel and 27 percent in concrete when composite construction is used. Soil-cement backfill could be used from the bonded bedding termination to the spring line.

Dramatic savings may be realized for larger conduits. Consider a pipe. In a narrow trench, a conduit with a 5½-in. (140-mm) core and 120 deg of bonded bedding 3½ in. (89 mm) thick should support more than 13 ft (4 m) of 110-lb/ft^3 (1762-kg/m^3) backfill without reinforcement. For 13 ft (4 m) of fill, conventional design of the C 76 B-walled pipe with class B bedding would need 1,100-D (52.7-D_{SI}) pipe that has a steel area of at least 0.59 in.^{2}/ft (12.7 cm^2/m). Composite construction even in a reconstructed trench with a lateral support value of 0.33 would only require 0.44 in.^{2}/ft (9.5 cm^2/m) of steel. If q were 0.67, A_s would be 0.22 in.^{2}/ft (4.7 cm^2/m).

The lighter cores can be transported and hauled at less cost. There would be savings in excavating and backfilling less material, less even than in most conventional pipe trenches, and savings in materials and labor when select bedding is prepared. Partially offsetting these savings is the cost of pouring about 0.1 yd^3 (0.076 m^3) of soil-cement/ft of conduit. For a simple comparison, the excavation and backfill and the total concrete and steel required for the 108-in. (2743-mm) composite pipe would be about the same as for the ASTM C 76, 84-in. (2134-mm) class I-walled B pipe.

TESTS

To verify many of these theories, field tests were conducted by Hydro Conduit Corporation in Phoenix in 1973 on eight sections of pipe that represented the five designs shown in Figures 8, 9, 10, 11, and 12. Figure 13 shows a sectional view of the installation (7).

Construction of the pipeline is shown in Figures 14, 15, and 16.

On January 8, 1973, 20 days after installation field loading, tests were conducted on the eight sections of the pipeline in the order shown in Figure 13. The method of loading was to center a 126-in.-wide (3200-mm) by 20-ft-long (6.1-m) steel cylinder over the section to be tested and to fill the cylinder with sand as shown in Figure 17. Measurements were taken and recorded of horizontal and vertical deflection of the pipe simultaneously at both ends of the section being tested after each 2 ft (0.61 m) of overburden were placed.

Each pipe had approximately 2 ft (0.61 m) of backfill to ground level before the cylinder was placed over the pipe except for pipe D-1 (Figure 13) in test 2, which started with about 4 ft (1.2 m) of initial cover.

Test sections had a maximum fill of about 23 to 25 ft (7 to 7.6 m). The steel cylinder weighed approximately 6 tons (5443 kg) so that the total maximum load on each test section area was about 106 tons (96 200 kg). The unit stress at the top of the pipe itself was about 2,450 lb/ft^2 (117 kPa). The total load on an 8-ft (2.4-m) length of pipe was 58.5 tons (53 000 kg) and the D-load was 2,930 (140 D_{SI}). Test section 2 (pipe D-1) had 2 ft (0.61 m) more fill or a total load of 115 tons (104 000 kg) and a D-load of 3,200 (153 D_{SI}).

The diameter changes were measured by reading the scales of Ames dials. These were attached between telescoping rods, which were held continuously by springs to marbles that were attached to the walls of the pipe about 1 ft (0.3 m) from each end as shown in Figure 18.

Micrometer readings were also taken between marbles before and after each test, but alignment problems probably made them less reliable than the Ames readings.

Figure 8. Thin-walled pipe with soil-cement backfill used in Phoenix test installation.

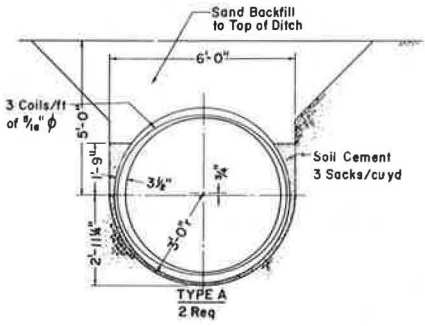

Figure 9. Grooved composite test pipe bonded at top and bottom with 1¾-in. (44.5-mm) overlay bonded at top and bottom.

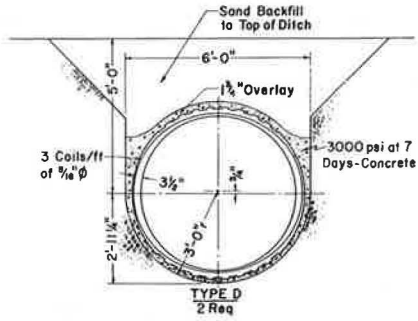

Figure 10. Grooved composite test pipe bonded at top and bottom with 3½-in. (89-mm) overlay bonded at top and bottom.

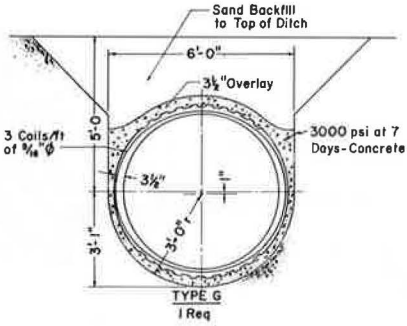

Figure 11. Overlays of 3½ in. (89 mm) on ungrooved thin-walled test sections.

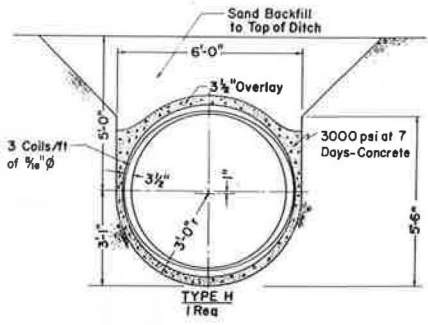

Figure 12. Control test section with 5¼-in. (133.4-mm) wall and sand backfill.

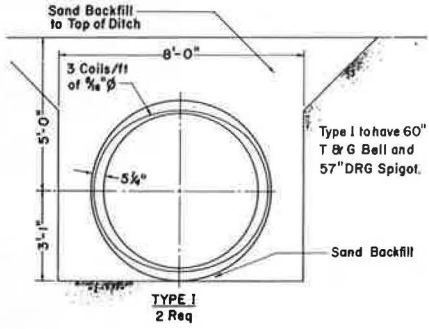

Figure 13. Flexible joint details and test pipeline profile.

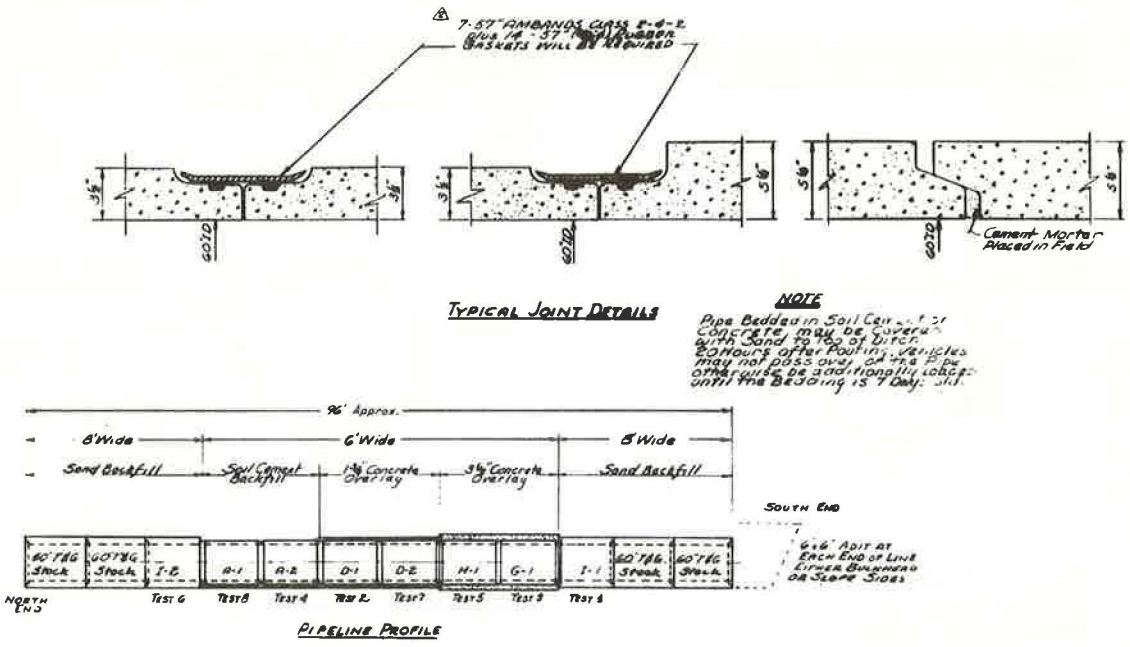

Figure 14. Template for rounded trench bottom for Phoenix tests.

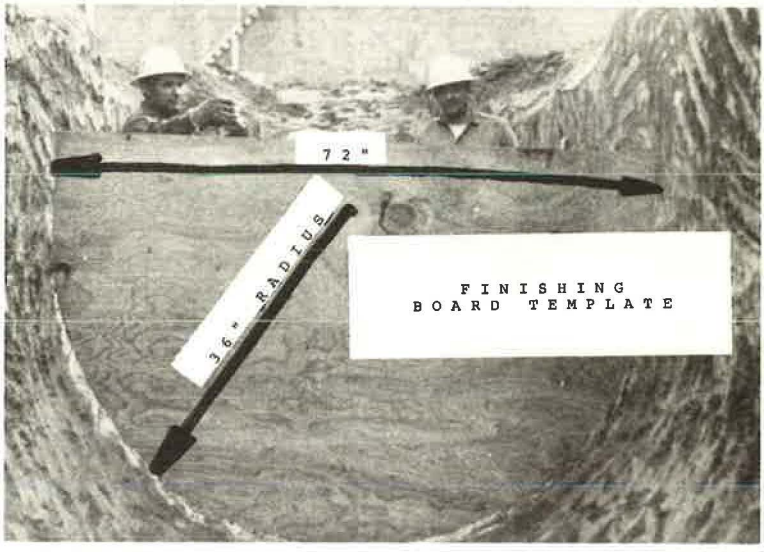

Figure 15. Concrete blocks used to position test sections in narrow trench.

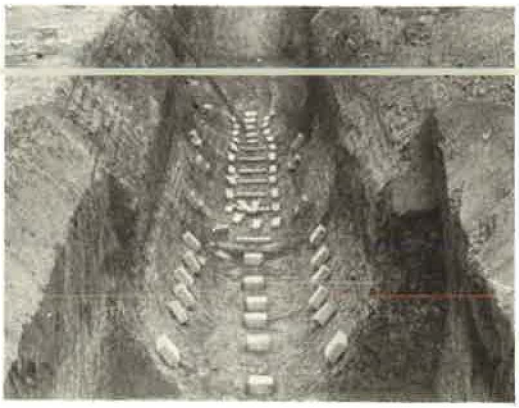

Figure 16. Phoenix test sections with bulkheads separating segments prior to backfilling.

Figure 17. Sand being dropped into 126-in. (3200-mm) cylinder centered over alternate test sections to simulate field load.

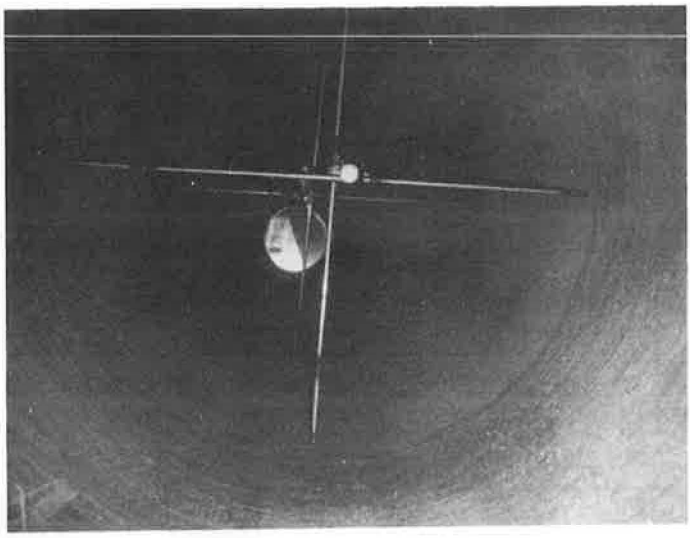

Figure 18. Dial gauges used to measure horizontal and vertical deflections of each test section during loading sequence.

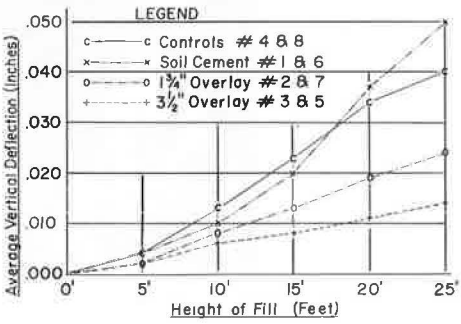

Figure 19. Average vertical deflections of four conditions of test pipes under various heights of backfill.

Table 2. Vertical deflections of test conduits under 20 ft (6.1 m) of fill.

California DOT Test	Δ[a]	Other Tests	Δ[a]
Zone 7	0.0012	ACPA trench	0.0019
Zone 8	0.0008	ACPA embankment	0.0008
Zone 9	0.0025	Phoenix control	0.0006
Zone 10	0.0015	Phoenix soil-cement	0.0006
Zone 11	0.0009	Phoenix 1¾-in. overlay	0.0003
Zone 12	0.0034	Phoenix 3½-in. overlay	0.0002

Note: 1 in. = 25.4 mm.

[a]Deflections in inches (millimeters) are divided by pipe diameter in inches (millimeters) and thus are nondimensional for comparisons.

Vertical deflections are shown in Figure 19 for incremental loadings. The values have been averaged for ease of comparison.

These tests prove that composite as opposed to conventional construction will greatly limit deflections. Just how small these deflections are is more apparent when they are compared with deflections measured in the California DOT 84-in. (2134-mm) test pipeline at Mountainhouse Creek (8) and the American Concrete Pipe Association (ACPA) test lines in Ohio. Table 2 gives deflections divided by diameter for 20 ft (6.1 m) of fill.

Table 2 data indicate that the dense sand backfill used for the control section at Phoenix was about as favorable a material as could be chosen. Therefore, deflections were only 17 to 80 percent of any of the other conduits. These comparisons are relative because the Phoenix tests were in a trench although most of the others were in embankments.

Compared with this most favorable trench installation, the composite conduits deflected only 22 and 44 percent as much under 20 ft (6.1 m) of backfill.

CONCLUSIONS

Composite construction can offer economic savings in concrete pipe type conduits. Many such conduits, even under high fills, do not require structural reinforcement when installed in narrow trenches. Even in formed trenches and in designs without lateral support, composite conduits can greatly reduce required concrete and steel.

Designs for unreinforced and reinforced conduits differ. Thickened walls in selected areas of unreinforced conduits stiffen these sections and attract moments, but the ability of the section to resist moment is proportional to the square of the wall thickness. However, steel areas in reinforced conduits vary directly with moment arms.

Conduits bonded at the bottom for open construction and at the top and bottom for closed construction currently seem to be the most feasible to manufacture and install. Consideration should be given to thickening side portions of core units or to applying reinforced structural concrete at the side portion of the envelope for further economic savings.

Analyses and field tests of thin-cored composite conduits in narrow, natural, or artificial trenches verify theories that will be useful in obtaining more reliable and economical composite conduits for almost any fill of normal height.

ACKNOWLEDGMENT

I am indebted to numerous people who have contributed to these efforts including C. Mack Albertson; E. D. Dowden, Jr.; K. K. Kienow; L. M. Johnson; J. Devine; M. W. Piché; J. P. Zicaro; W. Franz; and, in particular, Wayne W. Smith, who developed the computer program for the analyses.

REFERENCES

1. H. C. Pettibone and A. K. Howard. Distribution of Soil Pressures on Concrete Pipe. ASCE Water Resources Engineering Conference, Denver, May 1966.
2. D. C. Etheridge. Soil Cement Slurry Cuts Pipelaying Steps. Construction Methods and Equipment, Vol. 54, No. 10, Oct. 1972, pp. 88-89.
3. What About Non-Reinforced Precast Concrete Pipe? California Engineer and Builder, July 28, 1972.
4. M. L. Johnson. Concrete Beam Test Program. Hydro Conduit Corp., Oct. 15, 1974.
5. W. W. Smith. Analysis by Computer of Variable Wall Pipes (or Rings). Hydro Conduit Corp., Oct. 1974.
6. W. W. Smith. Deflections and Lateral Loads. Hydro Conduit Corp. for ASCE Seminar on Lateral Pressures on Large Pipe, Tunnels and Caissons, Oct. 1974.

7. T. K. Breitfuss. Composite Installed Pipe. Hydro Conduit Corp., March 15, 1973.
8. R. E. Davis and A. E. Bacher. Structural Behavior of a Concrete Pipe Culvert—Mountainhouse Creek (Part 1). Division of Highways, California Department of Transportation, Rept. 4-71, April 1971.

DISCUSSION

M. G. Spangler, Engineering Research Institute, Iowa State University

The thesis of this paper and the ideas expressed are the most innovative that I have encountered in approximately 50 years of activity and observation in the field of buried conduit design and installation. Although I may have some mental reservations relative to the practical aspects of both the manufacture and installation of the composite structures, nevertheless it is refreshing and valuable to have these ideas laid out and made available for discussion. This is particularly true since Breitfuss has wide experience in the concrete pipe manufacturing industry and has the point of view of a businessman and a competent engineer.

I have had occasion to investigate the structural failure of several dozen buried pipelines and, in each case, have attempted to pinpoint the most probable cause or causes of the failure. Each individual case had its own peculiar circumstances that might have contributed to the difficulty, but two conditions are predominant: (a) the case of ditch conduits in which an actual width of the ditch at the elevation of the top of the pipe was greater than the width for which the pipe was designed and (b) the case of both ditch and projecting conduits in which a bedding condition produced a highly concentrated upward reaction on the bottom of the pipe and thus increased the bending moment in the pipe wall and decreased the supporting strength of the pipe.

The methods of pipe manufacture and installation depicted by Breitfuss in Figure 1 would go a long way toward alleviating the detrimental influence of both these adverse circumstances. For example, with respect to load on a pipe, it is widely recognized that the actual width of ditch at the elevation of the top of the pipe has an important influence on the load to which the pipe is subjected and which it must support without evidence of structural distress. The Marston equation, which is used extensively for determining loads on ditch conduits, is

$$W_c = C_d w B_d^2 \tag{9}$$

where

W_c = load on conduit in pounds/linear foot (newton/meter),
C_d = a load coefficient = $[(1 - e)^{-2K\mu'}(H/B_d)]/2K\mu'$,
w = unit weight of soil,
H = height of fill above top of pipe,
B_d = width of ditch at elevation of top of pipe,
K = lateral pressure ratio (Rankine),
μ' = coefficient of soil friction, and
e = base of natural logarithms.

Since the width of the ditch has such a great influence on the load on the buried structure, the installation of a pipe in a ditch having the same width as the outside diameter (OD) of the pipe, as shown in Figure 1, represents the minimum possible load situation in a given soil and under a given depth of cover. This can be demonstrated by calculating the load on 60-in. (1524-mm) pipes under 15 ft (4.6 m) of cover in ditches of various widths ranging from that of the 72-in. (1829-mm) pipe to that of the OD pipe

plus 60 in. (1524 mm). The latter width provides a 2½-ft (0.8-m) clearance on each side of the pipe. The results of such calculations are shown in Figure 20. They indicate that the load on a 72-in. (1829-mm) OD pipe in a ditch that is the same width as the pipe is only 47 percent of the load on the same pipe in an 11-ft-wide (3.4-m) ditch—a dividend certainly worth striving for.

Generally, the vertical earth load on the top of a buried pipe is approximately uniformly distributed over its full width. In contrast, the distribution of the equal and opposite reaction on the bottom of the pipe is influenced by the character and quality of the pipe bedding. Therefore, the stress in the pipe wall and its ability to support load vitally depend on the bedding. To illustrate this principle, consider a simple beam loaded variously as shown in Figure 21. For a load concentrated at the midspan, the bending moment is a maximum and equal to

$$M = 0.250\ Pl \tag{10}$$

where

M = maximum moment at centerline of span,
P = load, and
l = span length.

If the same magnitude of load is distributed uniformly over the span length, the maximum moment is

$$M = 0.125\ Pl \tag{11}$$

or only one-half the concentrated load moment.

For an intermediate distribution of load, say, over the middle third of the span, the moment is

$$M = 0.208\ Pl \tag{12}$$

This example from sophomore engineering mechanics of a simple beam is pertinent because exactly the same principle applies to a circular structure, such as a pipe, and the stress in the pipe wall is directly related to the distribution of the upward reaction on the bottom of the pipe. The function of good-quality bedding is to distribute the reaction as widely as possible and thereby reduce the bending moment stress.

To demonstrate further, I can indicate the bending moment at the bottom of the pipe when the width of bedding is expressed in terms of the central angle subtended by the effective bedding contact, as shown in Figure 22. The moment at the bottom is a maximum when the reaction is a concentrated load, e.g., when $\phi = 0$. It decreases rapidly as ϕ and the width of bedding increase, up to a value of about $\phi = 90$ deg. The benefit derived by increasing the bedding angle from 90 to 180 deg is relatively minor.

The importance of good distribution of the bottom reaction was brought to my attention in a recent investigation. A large-diameter sewer line constructed of reinforced concrete pipe had failed extensively in the invert. Interviews with the contractor and the engineer revealed that the pipe bedding consisted of 6 in. (152 mm) of compacted coarse, harsh gravel overlying shale bedrock. This bedding material was not shaped to fit the contour of the pipe. Rather, the pipe was laid on a flat surface of the gravel. There is little doubt that the bottom reaction was concentrated over a very narrow longitudinal element of the pipe and thus caused high bending moment and failure in the invert.

Figure 20. Load on 60-in. (1524-mm) pipe in ditches of various widths.

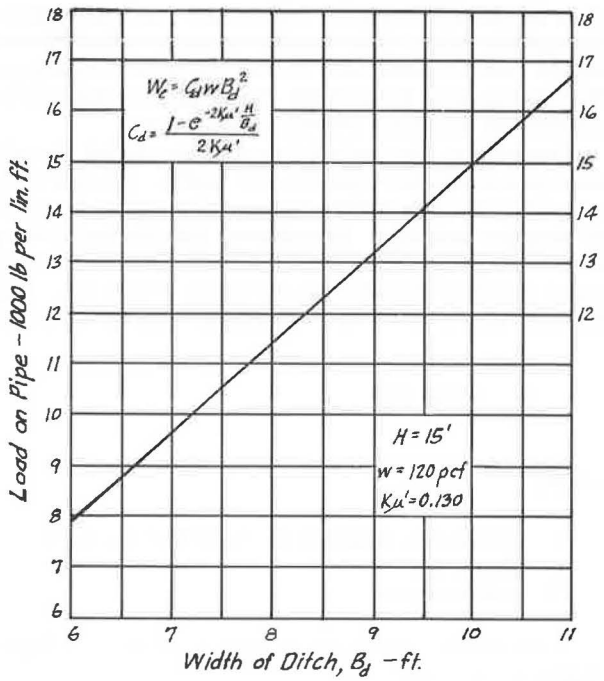

Figure 21. Influence of load distribution on bending moment.

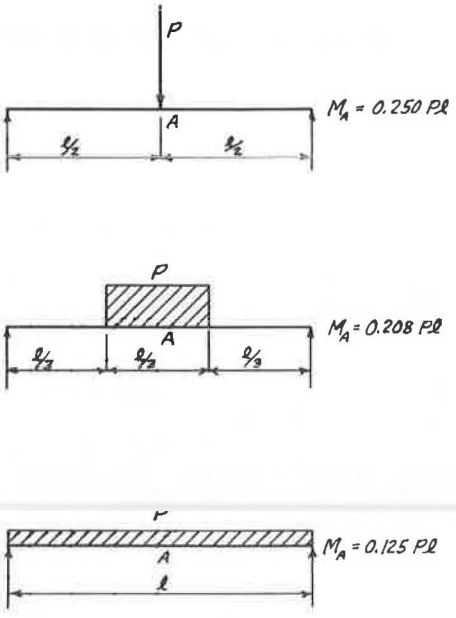

Figure 22. Influence of width of bedding on bending moment at B.

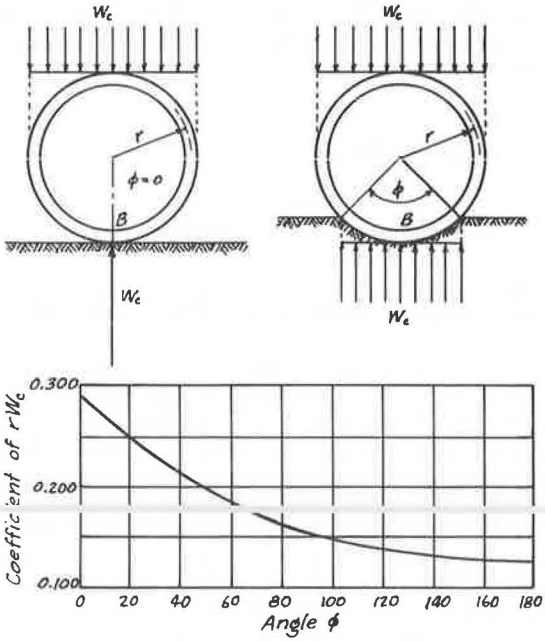

The foregoing discussion indicates that the prospective dividends, in terms of reduced stress in the wall of a buried conduit, brought about by the method of manufacture and installation recommended by Breitfuss are great. However, although I am not an expert in conduit construction, I have seen enough jobs being installed to be somewhat skeptical of the practicality of the proposals under current conditions of contractual relations in this field. All too often, a general contractor does not have the knowledge or appreciation of the importance of accurate control of excavation, adequate bedding, and good backfilling practices and is understandably cost conscious and much interested in maintaining a satisfactory production schedule. Furthermore, guidance and direction by the engineer in charge often leave much to be desired. In some instances when a pipeline gets in trouble, the contractor and the engineer may get their heads together and jump to the conclusion that faulty pipe was the cause of a failure, when nearly always it is poor-quality installation that is the culprit.

There is need for major upgrading of installation practices in the field of conduit engineering, and the proposals outlined by Breitfuss would appear to go a long way toward that end, if such proposals are faithfully carried out. In this connection, Breitfuss suggests that a distinct advantage might accrue if pipe manufacturers accepted responsibility for the installation of a buried pipeline and its manufacture and delivery to a site. Some type of turnkey contract between the manufacturer and the contractor might be worked out, and the result would be that installation crews in the employ of the manufacturer would install the pipe and backfill it to the top. Or as an alternative, the manufacturer might furnish expert supervision of the bedding and backfilling operations. In either case, it is believed that better results would be attainable than under the current system of divided responsibility between the supplier and the contractor.

AUTHOR'S CLOSURE

I value and agree with the comments by Spangler. I appreciate his expanded discussion on two important aspects of the concept: the reduced load on the pipe and the practical application of this type of construction.

My paper may be said to deal primarily with design and economic comparison for lower costs; Spangler's discussion is more related to improved performance.

Spangler offers a good simple illustration of load and moment reductions when an ensured wider supporting base is used. Although it is true that increasing the bedding angle from, say, 120 to 180 deg decreases invert moments only 8 to 10 percent, continuous support for 180 deg prevents high stresses from developing where bedding changes abruptly from rigid to yielding [series C (1), zone 10 (6)]. The reader must also realize the importance of ensured lateral support when 180-deg bedding is used. Increasing side support from, say, 33 to 67 percent of the vertical load decreases moments about 50 percent. The composite pipe in the Phoenix tests (7) should support more than 40 ft (12.2 m) of fill without cracking.

Spangler has some reservations on the manufacture and installation of composite structures. In relation to manufacture, there are probably minor economic advantages in a small pipe, but there are now several methods of making larger concrete cores. Cores can be made on packerhead or dry-cast machines with slightly thinner walls, standard joints, and much less reinforcement. Slots or ridges can be formed in the core units when they are made. Much thinner walled cores can be made by the centrifugal or wet-cast process. With certain modifications these processes can also make cores with thicker sides to maximize the advantages of composite construction. For example, tunnel liners with thickened side walls can be reinforced elliptically so that moments will be balanced in the composite structure after grout backfilling in a much smaller tunnel than is currently required [4 in. (102 mm) in a 10-ft (3-m) tunnel represents 7 percent less excavation]. Another major application is an alternative to large monolithic or box culverts.

Three factors for additional development as mentioned by Spangler are economical joints, reliable side support verification, and machinery to install composite conduits.

One machine mentioned in the paper is under development to hold cores in position while concrete or other types of backfill are placed beneath or around them. The ingenuity of contractors and construction machinery manufacturers should result in more efficient installation machines. However, Spangler appropriately suggests more defined responsibilities for installation. A composite conduit is decidedly a soil-structure system whose success depends on both components of the system. Correct construction is somewhat self-governing in that, if the subgrade and invert are correct, the composite wall at the bottom will be correct. Besides, the installer wants the narrowest possible trench to save materials. Forming and holding that trench may cause disputes between the trenching contractor and the conduit installer acting as a subcontractor, but these disagreements can probably be resolved contractually.

FAILURE OF A CAST-IN-PLACE UNREINFORCED CONCRETE CONDUIT

Jerry C. Chang, Division of Construction and Research,
California Department of Transportation

A case history of the failure of a 72-in. (183-cm) cast-in-place, unreinforced concrete conduit constructed near the toe of a highway embankment is described. Theoretical analysis was conducted to predict the behavior of the conduit. It was concluded that the conduit had failed primarily because of the additional lateral load exerted by a 70-ft-high (21.3-m) embankment. The effectiveness of the theoretical analysis was demonstrated by using actual conduit failure.

•IN September 1969, a 72-in. (183-cm) cast-in-place, unreinforced concrete drainage conduit was placed at the toe of an embankment before the embankment was constructed in the I-10, 57 interchange near San Dimas, Los Angeles County, California (Figure 1). The pipe was constructed by excavating a trench with vertical sides and a semicircular bottom. Forms were then placed in the trench, and the lower half of the pipe was cast first. The forms were then stripped and placed on top of the cast section, and the upper half of the conduit was then poured. The completed conduit has a thickness of 6 in. (15.2 cm). Moderate patching was performed on the interior surface and the exterior surface of the upper half of the conduit. Tests of concrete cylinders indicated an average 28-day compressive strength of 4,490 psi (30 960 kPa).

In October 1969, the trench was backfilled with the previously excavated material and compacted to 90 percent relative compaction. When the backfilling operation was completed, a visual inspection of the conduit revealed no interior cracking or damage.

In April 1970, the highway embankment adjacent to the conduit (Figure 2) was then placed to a height of 20 ft (6.1 m). Another inspection of the conduit indicated no distress. In October through November 1970, the embankment was completed to a height of approximately 70 ft (21.3 m).

In January 1971, a third inspection of the conduit showed extensive cracking, particularly along the spring line of the conduit. The top half of the conduit was laterally displaced away from the embankment by as much as 3 in. (7.6 cm) relative to the bottom half.

Figures 3 and 4 show the crack in the conduit along the spring line and the crown respectively.

SOIL AND FOUNDATION CONDITIONS

When the damage of the conduit was discovered, undisturbed soil samples were taken from boring holes A, B, and C along the conduit (Figure 1). The log of borings showed a moist, silty clay to clayey silt for a depth of approximately 8 ft (2.4 m), a sand layer at 8 to 11 ft (2.4 to 3.4 m), and then silty clay to a depth of 18 ft (5.5 m) (Figure 2). Triaxial compression tests were conducted to determine the shear strength of the soil sample under unsaturated, unconsolidated, and undrained conditions. The test results are given in Table 1.

Publication of this paper sponsored by Committee on Subsurface Structures Design.

Figure 1. Drainage pipe layout.

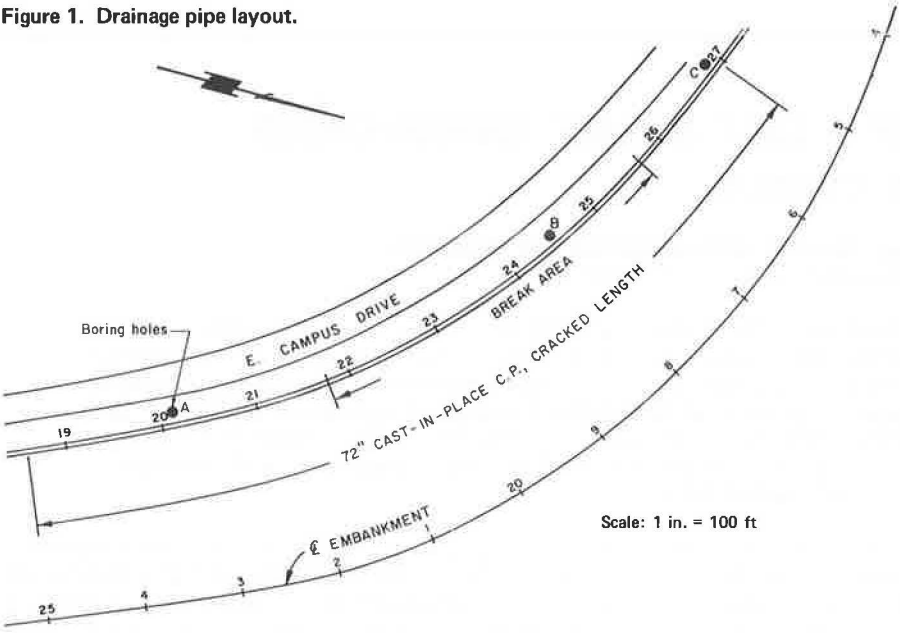

Figure 2. Typical embankment section.

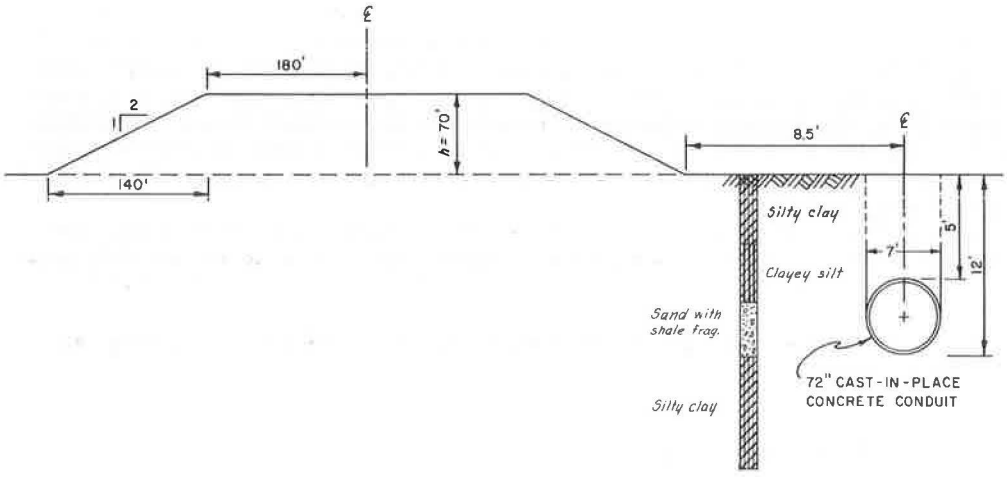

Table 1. Triaxial compression test results.

Depth of Boring (ft)	Soil Type	Wet Unit Weight (lb/ft^3)	Cohesion (lbf/ft^2)	Angle of Internal Friction (deg)
0 to 6	Silty clay	108 to 111	1,200	0
6 to 8	Clayey silt	111 to 124	800	14
8 to 11	Sand with shale fragments	113 to 120	0	34
11 to 18	Silty clay	115 to 118	1,600	10

Note: 1 ft = 0.3 m. 1 lb/ft^3 = 16.02 kg/m^3. 1 lbf/ft^2 = 47.9 Pa.

THEORETICAL ANALYSIS

A theoretical analysis was conducted to determine the stresses developed in the conduit wall because of the local overburden and the load transferred from the highway embankment.

Earth Pressure on Conduit Due to Local Overburden

The vertical earth pressure P_z and the horizontal earth pressure P_x acting on the conduit from the local overburden were computed as follows:

$$P_z = \frac{C_d \gamma B^2}{B} = C_d \gamma B \tag{1}$$

$$P_x = K_o \gamma h \tag{2}$$

where

γ = unit weight of the backfill soil,
B = width of trench,
C_d = load coefficient for ditch conduit,
K_o = coefficient of earth pressure at rest, and
h = height of overburden at section in question.

Equation 1 is based on the equation developed by Spangler for load on a ditch conduit (1). The value of C_d was estimated to be 0.7 from Spangler's chart. Equation 2 is the general equation for estimating earth pressure at rest.

According to Jaky (2),

$$K_o = 1 - \sin\phi \tag{3}$$

where ϕ is the internal friction angle of the soil. Table 2 gives the internal friction angle of the foundation soils. For simplicity in the computation, the K_o value was assumed to be unity in the analysis. The unit weight of soil was estimated to be 135 lb/ft^3 (2160 kg/m^3).

Earth Pressure on Conduit Due to Highway Embankment Load

The earth pressure on the conduit due to the embankment load was estimated for computing subsoil stress at any point A in the foundation soil due to a trapezoidal embankment loading. This pressure was estimated from the equation given by Chang (3), where γ = unit weight of the embankment soil and horizontal stress is

$$\sigma_x = \frac{P}{\pi a}\left[a(\theta_1 + \theta_2 + \theta_3) + B(\theta_1 + \theta_3) + X(\theta_1 - \theta_3) - 2Z\log_e\frac{R_1R_4}{R_2R_3}\right] \tag{4}$$

and vertical subsoil stress is

Figure 3. Cracks in conduit at spring line.

Figure 4. Cracks in conduit at crown.

Figure 5. Subsoil stresses under symmetrical trapezoidal load.

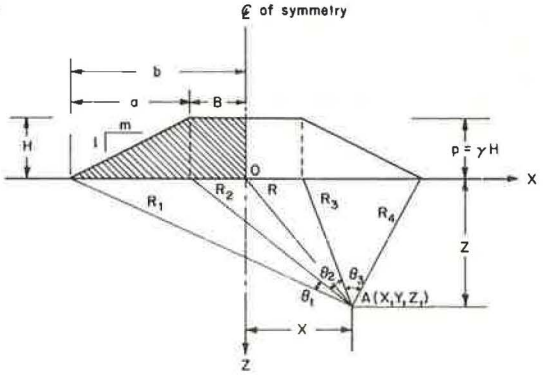

Figure 6. Load of external soil pressure on conduit.

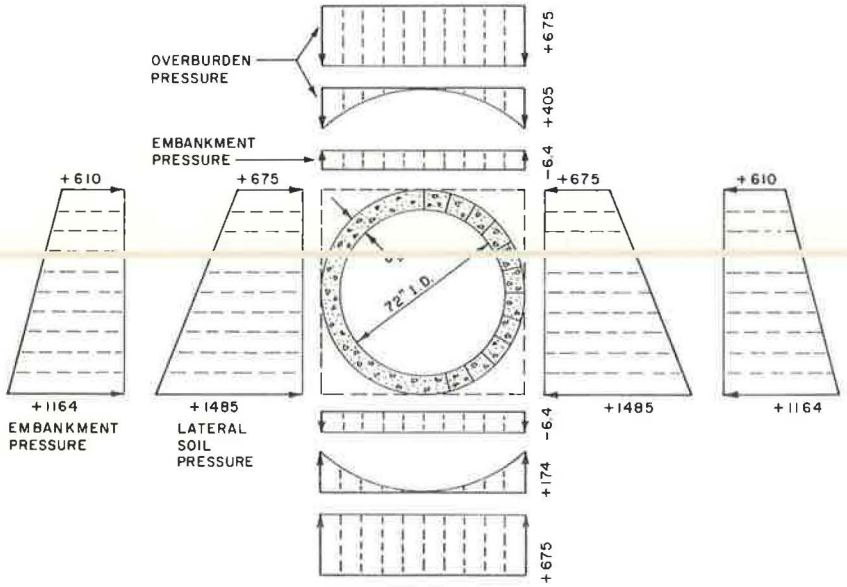

$$\sigma_z = \frac{P}{\pi a}\left[a(\theta_1 + \theta_2 + \theta_3) + B(\theta_1 + \theta_3) + X(\theta_1 - \theta_3)\right] \quad (5)$$

The stresses under a symmetrical trapezoidal load are shown in Figure 5. The loading of the external soil pressure [pounds/foot^2 (pascal)] on the conduit is shown in Figure 6.

Internal Hydrostatic Pressure

When the conduit is flowing full with water, hydrostatic pressure [pounds/foot^2 (pascal)] would act on the internal face of the conduit. The distribution of the water pressure is shown in Figure 7.

Structural Analysis

Structural analysis of the moment, thrust, and shear developed in the conduit wall because of external and internal loads were computed by using the method developed by Phillips and Allen (4). They developed coefficient charts for moment, thrust, and shear for eight shapes of single-barrel conduit by means of Beggs Deformeter apparatus.

The results of moment, thrust, and shear tests are given in Table 2 for external loads and in Table 3 for the combination of external and internal loads. Figures 8, 9, and 10 show the moment, thrust, and shear developed in the conduit wall.

Stress analysis based on the computed result of the moment, thrust, and shear was conducted by using the equation developed by Zanger (5) as follows:

$$\sigma_1 = \frac{1}{2d}\left\{T + \frac{12\ My}{d^2} + \sqrt{\left(T + \frac{12\ My}{d^2}\right)^2 + 9S^2\left[1 - \left(\frac{2y}{d}\right)^2\right]^2}\right\} \quad (6)$$

$$\sigma_2 = \frac{1}{2d}\left\{T + \frac{12\ My}{d^2} - \sqrt{\left(T + \frac{12\ My}{d^2}\right)^2 + 9S^2\left[1 - \left(\frac{2y}{d}\right)^2\right]^2}\right\} \quad (7)$$

$$\tan 2a = 3S\left(\frac{d^2 - 4y^2}{Td^2 + 12\ My}\right) \quad (8)$$

$$\tau_{max} = \frac{1}{2}(\sigma_1 - \sigma_2) \quad (9)$$

where

T = thrust force,
S = shear force,
M = moment,
d = wall thickness of conduit,
x,y = rectangular coordinates,
σ_1, σ_2 = principal stresses,
τ_{max} = maximum shear stress, and
α = angle of orientation of principal stress measured clockwise from x-axis.

Figure 7. Hydrostatic pressure on internal face of conduit.

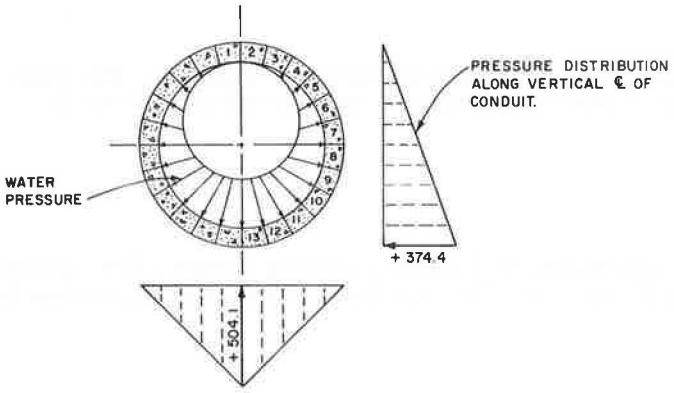

Table 2. Moment, thrust, and shear due to external load.

Section	Moment (lbf-in./in.)	Thrust (lbf-in.)	Shear (lbf-in.)
1	-3,043	+504	0
2	-2,676	+488	-75
3	-1,647	+446	-132
4	-190	+383	-161
5	+1,360	+316	-152
6	+2,612	+261	-101
7	+3,227	+1,385	-20
8	+2,989	+256	+76
9	+1,888	+326	+159
10	+168	+432	+202
11	-1,685	+549	+188
12	-3,103	+639	+112
13	-3,639	+673	0

Note: 1 lbf-in./in. = 4.45 N·m/m. 1 lbf-in. = 0.1130 N-m.

Table 3. Moment, thrust, and shear due to internal and external loads.

Section	Moment (lbf-in./in.)	Thrust (lbf-in.)	Shear (lbf-in.)
1	-2,625	+473	0
4	-94	+361	-143
7	+2,841	+1,375	-13
10	+102	+408	+173
13	-2,990	+610	0

Note: 1 lbf-in./in. = 4.45 N·m/m. 1 lbf-in. = 0.1130 N-m.

Figure 8. Moment in conduit wall.

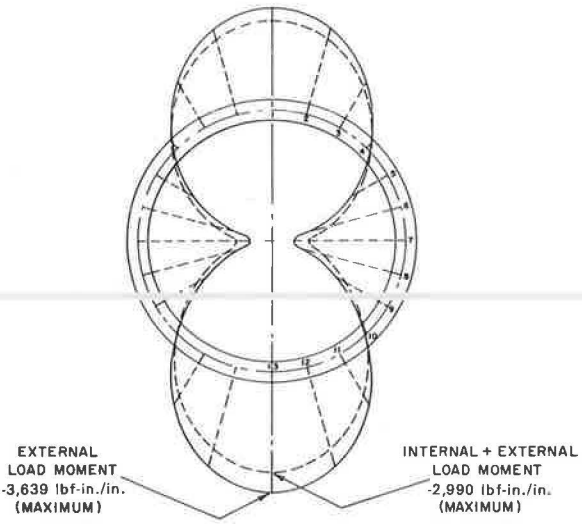

Scale: 1 in. = 3,000 lbf-in./in.

Figure 11 shows the sections cut radially along the wall of the conduit for stress analysis and the relationship among parameters in equations 6, 7, 8, and 9. The analyzed results of principal stresses due to external earth pressure are given in Table 4, and those due to internal water pressure are given in Table 5.

Tensile stresses of more than 400 psi (2760 kPa) developed at the exterior face of the conduit at the top and bottom of the wall (sections 1 and 13), and stresses of more than 300 psi (2070 kPa) developed at the interior face of the wall at the spring line (section 7) (Table 4). A maximum shear stress approaching 400 psi (2760 kPa) developed in the wall at the spring line of the conduit. The computed allowable tensile stress is 217 psi (1496 kPa), and the allowable shear stress is only 113 psi (779 kPa) based on the average 28-day strength of 4,490 psi (30 960 kPa). These stresses are based on the formula given in the 1973 American Concrete Institute Manual of Concrete Practice. Figure 12 shows the locations of the potential cracks in the conduit wall based on the theoretical results of the high tensile stresses.

CONCLUSIONS

Visual inspection, backed by theoretical analysis, indicates that the failure of the conduit was primarily due to the additional lateral load exerted by the 70-ft-high (21.3-m) embankment located about 8.5 ft (2.6 m) away from the conduit. The conduit was cracked first at the inner face along the spring line (also the location of the construction joint). The upper half of the conduit was then sheared off and displaced by as much as 3 in. (7.6 cm) away from the embankment by the lateral earth pressure exerted from the embankment load. Since the lower half of the conduit was cast neatly in the excavated, semicircular-shaped trench, which was mostly composed of sandy soil with shale fragments and was more rigid than the clayey backfill material surrounding the top of the conduit, it was held in place without appreciable movement.

There was no circumferential crack observed on the conduit wall. Therefore, it can be concluded that there was no appreciable uneven settlement along the axis of the conduit. This conduit was replaced with a class 4, double-caged, reinforced concrete pipe after the conclusion of this study in June 1971.

This case history points out the necessity of considering the effects of loads adjacent to the conduit trench as well as those directly over the conduit. The analyzed results have verified the conduit failure and have accurately predicted the locations of cracking of this conduit. I am currently making additional analyses using finite element method and assuming the beam element to be the conduit wall. These results will be reported on in the future.

ACKNOWLEDGMENT

This study was performed for the culvert committee of the California Department of Transportation under the direction of Raymond A. Forsyth. The conduit was constructed under the supervision of Transportation District 07. Particular thanks are extended to District Materials Engineer, J. T. Webster, and Resident Engineer, R. Noad, who provided invaluable information for this paper. Ellsworth L. Chan and Christopher J. Masklee of the Geotechnical Branch, Transportation Laboratory, assisted in the theoretical analysis and preparation of this paper.

REFERENCES

1. M. S. Spangler. Soil Engineering. 1960, pp. 399-401.
2. J. Jaky. Pressure in Silo. Proc., International Conference on Soil Mechanics and Foundation Engineering, Rotterdam, 1948.
3. J. C. Chang. Foundation Stability of Highway Embankments Founded on Deep Clay Soil. Louisiana State Univ., Baton Rouge, Master's thesis, 1964, p. 12.

Figure 9. Thrust in conduit wall.

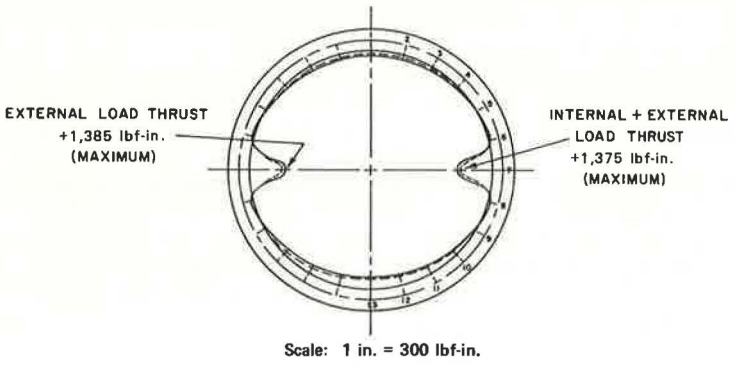

Figure 10. Shear in conduit wall.

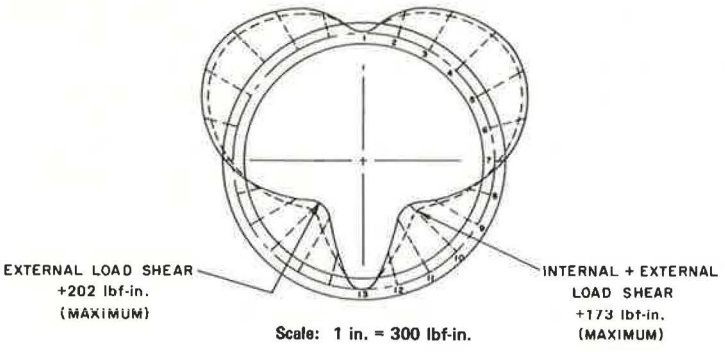

Figure 11. Sections cut radially along conduit wall and relationship among parameters for stress-analysis equations 6, 7, 8, and 9.

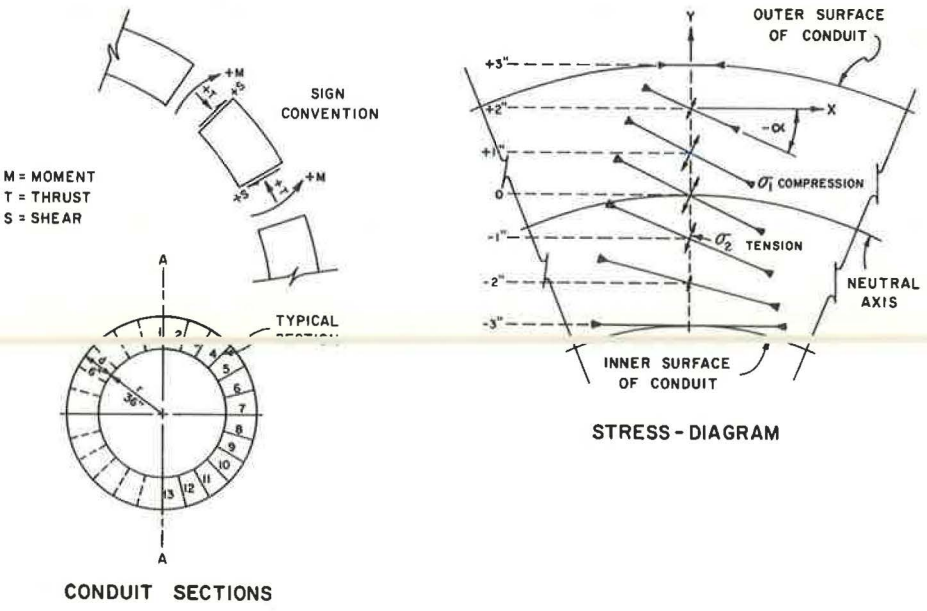

Table 4. Stresses due to external earth pressure.

Section	Y (in.)	σ_1 (psi)	σ_2 (psi)	τ_{max} (psi)	α (deg)
1	+3	0	-423	211	0
	+2	0	-254	127	0
	+1	0	-85	42	0
	0	+84	0	42	0
	-1	+253	0	126	0
	-2	+422	0	211	0
	-3	+591	0	295	0
4	+3	+32	0	16	0
	+2	+52	-9	31	-23
	+1	+71	-18	44	-27
	0	+83	-19	51	-26
	-1	+89	-14	52	-22
	-2	+91	-5	48	-14
	-3	+96	0	48	0
7	+3	+769	0	384	0
	+2	+589	0	295	0
	+1	+410	0	205	-1
	0	+231	0	116	-1
	-1	+52	0	26	-5
	-2	0	-128	64	-1
	-3	0	-307	154	0
10	+3	+100	0	50	0
	+2	+99	-8	53	+16
	+1	+101	-20	61	+27
	0	+98	-26	62	+27
	-1	+86	-23	55	+28
	-2	+65	-12	39	+23
	-3	+44	0	22	0
13	+3	0	-494	247	0
	+2	0	-292	146	0
	+1	0	-90	45	0
	0	+112	0	56	0
	-1	+314	0	157	0
	-2	+517	0	253	0
	-3	+718	0	359	0

Note: Stress sign convention, + = compression, - = tension.
1 in. = 2.5 cm. 1 psi = 6.89 kPa.

Table 5. Stresses due to internal water pressure.

Section	Y (in.)	σ_1 (psi)	σ_2 (psi)	τ_{max} (psi)	α (deg)
1	+3	+65	0	32	0
	+2	+41	0	21	0
	+1	+18	0	9	0
	0	0	-5	3	0
	-1	0	-28	14	0
	-2	0	-52	26	0
	-3	0	-75	37	0
4	+3	+12	0	6	0
	+2	+8	-1	4	+18
	+1	+5	-3	4	+39
	0	+3	-7	4	-34
	-1	+2	-11	6	-21
	-2	0	-15	8	-10
	-3	0	-20	10	0
7	+3	0	-66	33	0
	+2	0	-45	22	-1
	+1	0	-23	12	-4
	0	+1	-3	2	-33
	-1	+20	0	10	+5
	-2	+41	0	21	+1
	-3	+63	0	31	0
10	+3	0	-15	8	0
	+2	+1	-13	7	+18
	+1	+4	-11	8	+30
	0	+6	-10	8	+37
	-1	+6	-7	7	+44
	-2	+6	-3	4	-34
	-3	+7	0	4	0
13	+3	+98	0	49	0
	+2	+62	0	31	0
	+1	+26	0	13	0
	0	0	-11	5	0
	-1	0	-47	23	0
	-2	0	-83	41	0
	-3	0	-119	59	0

Note: Stress sign convention, + = compression, - = tension.
1 in. = 2.5 cm. 1 psi = 6.89 kPa.

Figure 12. Potential crack locations in conduit wall.

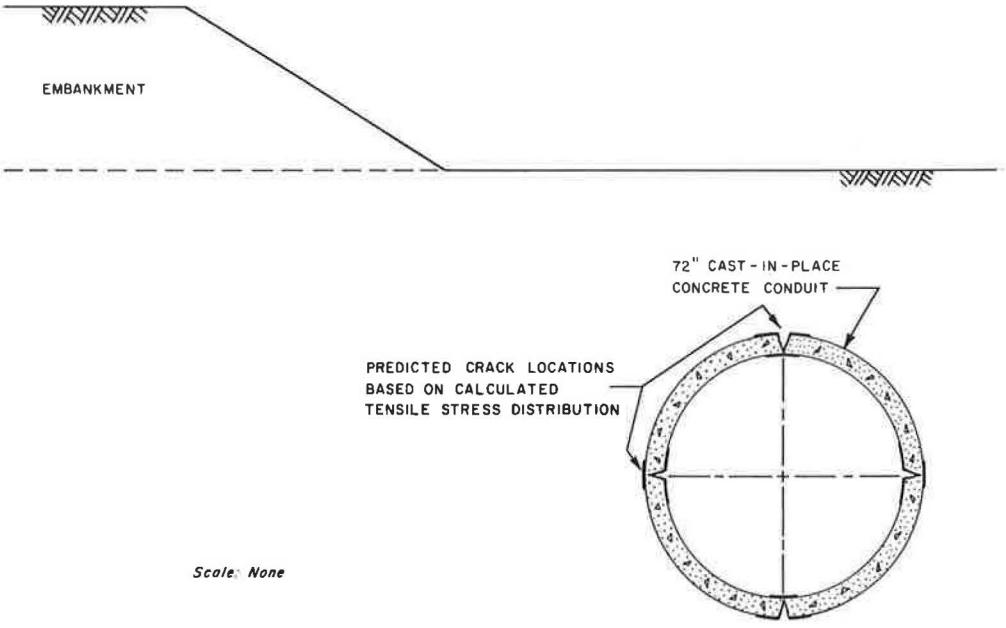

4. H. B. Phillips and I. E. Allen. Beggs Deformeter Stress Analysis of Single-Barrel Conduit. Bureau of Reclamation, U.S. Department of Interior, Denver, 1952.
5. C. N. Zanger. Analytical Determination of Principal Stresses in Structural Members. Bureau of Reclamation, U.S. Department of Interior, Denver, 1948, pp. 2-8.

WHERE ARE THE KINKS IN THE ALIGNMENT?

T. ten Brummelaar, School of Highway Engineering,
University of New South Wales, Australia

This paper uses the tangent method to determine the maximum length of an approach to a curve so that the driver does not see a kink (a sudden change in direction) in the alignment. Equations are presented for plan curves, crest curves, sag curves, and combinations of these curves. The picture presented by the road to the driver can be analyzed with the equations, and, thus, the road design engineer is able to relate important road properties to driver experiences. It is suggested that using this method to check road alignment design for kinks reduces the need for the time-consuming process of drawing perspectives.

•ANY curve, when seen from far away in perspective, looks like a sudden change in direction, a kink. This is even true for planned curves with large radii if they are observed from a long enough distance. At some distance, however, there is a transition between seeing the curve as a sudden direction change and seeing the curve as open, the critical distance. The kink does not give the driver sufficient information to accurately regulate the car's speed in anticipation of the curve to come. The development of the tangent method of drawing road perspectives has provided the road design engineer with many equations that allow analysis of the picture presented by the road to the driver. It allows a scientific means to relate important road properties to driver experiences. This method has been applied to find the maximum length of an approach to a curve so that the driver does not see a kink in the alignment. This knowledge can then be used to check road alignment design for kinks, and there will be a reduced need for the time-consuming process of drawing perspectives.

TANGENT METHOD

The tangent method (1, 2) assumes close similarity between circular curves on roads and parabolas. The perspective images of these parabolas have the form of hyperbolas. This allows the drawing of perspectives by a simple graphical method making use of the asymptotes of the hyperbola. One of the useful properties of the hyperbola is that the tangent point divides the tangent between the asymptotes into two equal parts (Figure 1, VP to T = T to H). Some other properties of a perspective image of a circular curve are shown in Figure 1 (distance D is shown at the reversal point). The equation follows from central projection theory and the parabolic assumption used in the tangent method.

The tangent method was used to draw all the perspectives in this paper and was found to be simple in its application, especially for road curves of large radii.

The notation used in the tangent method is as follows:

a = distance in meters from driver to road edge;
a_r = distance in meters from driver to road edge on driver's right;
A = clothoid spiral parameter, $LR = A^2$;

Publication of this paper sponsored by Committee on Geometric Design.

d = perspective viewing distance in meters (usually 1.0 m);
D = perspective distance in meters;
h = height in meters of the driver's eye above the pavement;
H = corner point, intersection between the tangent to the hyperbola at the terminal of the geometric element and the asymptote - 0;
M = midpoint, intersection of two asymptotes of a hyperbola;
R_H = radius in meters of horizontal circle or plan circle;
R_v = radius in meters of vertical circle;
R_{vc} = radius in meters of vertical crest curve;
R_{vs} = radius in meters of vertical sag curve;
T = terminal of geometric element;
V = speed of vehicle in kilometers per hour;
VP = vanishing point of direction at terminal of geometric element;
X = distance in meters on the road plan;
Y = level difference in meters on the road profile;
Z = total distance in meters from driver to point on road;
Z_1 = distance in meters from driver to terminal point of first geometric element; and
Z_2 = length in meters of second geometric road element.

DISTANCE OF REVERSAL POINT FROM DRIVER

It is assumed that drivers judge their expected speed-driving behavior for an oncoming curve by the visual shape of the reversal point formed by the inside curve edge of pavement (Figure 1). It is therefore of some value to the driver to be provided with an informative view of this reversal point at a distance. This allows the driver to draw conclusions and take action accordingly. This applies to circular, spiral, or parabolic curves in the vertical or horizontal direction.

A systematic analysis of the different situations follows.

PLAN CURVES

So that all possibilities can be covered fully, the curves are considered in groups:

1. Plan circular curves to the right,
2. Plan circular curves to the left,
3. Spiral curves, and
4. Plan circular curves on upslopes and downslopes.

Plan Circular Curves to Right

Plan circular curves to the right will be treated as the basic situation for the derivation of equations. The plan for such a situation is shown in Figure 1.

It is relatively simple to calculate the distance from a driver to the point where he or she sees the reversal in the inside curbline. This distance can be shown to be equal to Z, where

$$Z^2 = 2R_H a_r + Z_1^2 \qquad (1)$$

The derivation of equation 1 can be found in the Appendix.

With equation 1, it is possible to calculate the distance from a viewpoint to the place on the road edge where the driver sees the reversal curve. Where the driver is in fact already in the curved section,

$$Z_1 = 0$$

and the equation becomes

$$Z^2 = 2R_H a_r \tag{2}$$

This indicates a constant distance, as could be expected.

Plan Circular Curve to Left

The same equations as for plan circular curves to the right apply except that the distance a_r is replaced by a_l.

Spiral Plan Curves

For a clothoid spiral, the distance X as in Figure 1 would be approximately

$$\frac{Z_2^3}{6A^2} \tag{3}$$

and

$$D = \frac{a_r + \frac{-(Z - Z_1)^3}{6A^2}}{Z} \tag{4}$$

This equation cannot be reduced as simply as the equation for circular curves was. However, if the spiral is seen as a form between a straight line and a circular curve, it may be noted that for a straight line the reversal point lies at infinity.

For a circular curve, the reversal point lies at a constant distance from the beginning of the curve (equation 2). The spiral therefore must have its reversal point at a distance greater than the constant for the circular curve but less than infinity.

Driving toward a spiral presents the driver with a picture where the distance to the reversal point decreases to the circle constant. This provides the driver with a good optical guidance into the curve.

Plan Curves on Upslopes and Downslopes

From equations 1 and 2, note that the eye height of the observer does not have any effect on distance Z. It can also be shown that the actual perspective view of a sloping road is almost the same as that of a horizontal road because the distance of the vanishing points above or below the horizon is very small (Figure 2). Since the slope of the road is rarely steeper than 10 percent, the Y distances are practically less than 0.1 d. Arguments based on the idea that the observer looks against the road in the case of an upslope and with the road in the case of the downslope would favor total curve readability slightly in the case of the upslope. However, the improvement is so marginal that it can be neglected.

Figure 1. Plan and perspective view of road edge on right side of driver.

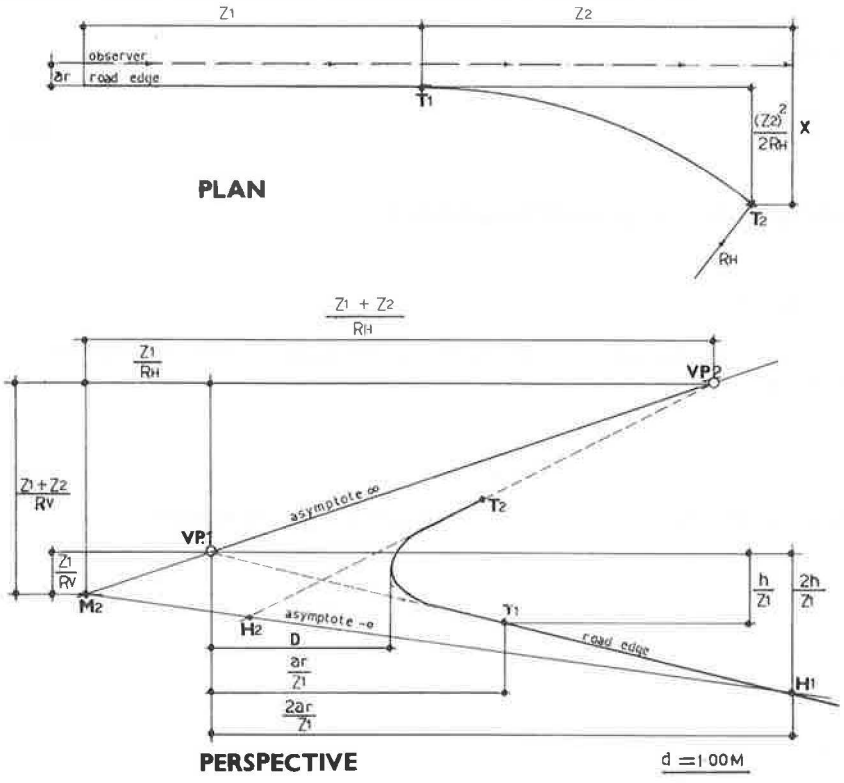

Figure 2. Perspectives of sloping roads as seen from same observation position.

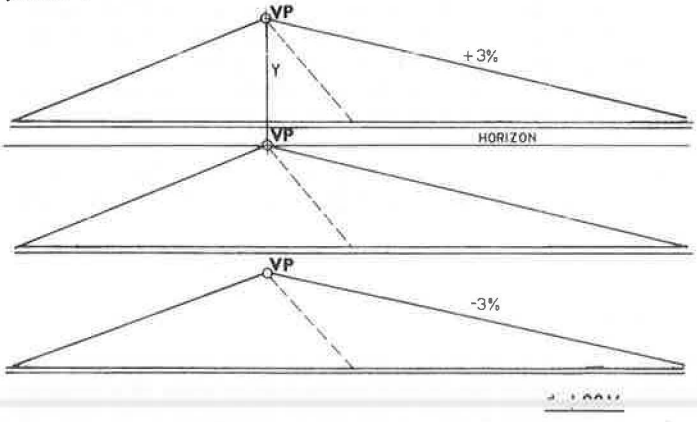

VERTICAL CURVES

Crest Curves on Straight Roads

The detailed analysis in the Appendix shows that, for crest curves (Figure 3), the distance from observer to the visible top of the crest equals Z, where

$$Z^2 = 2R_v h + Z_1^2 \tag{5}$$

This is of course similar to equation 1. The reversal point is in fact the visible top of the crest pavement.

Sag Curves on Straight Roads

In the sag curve there was no particular point that could be compared with the reversal point in the horizontal curve or with the top of the visible pavement at the crest. In fact, the total length of the pavement is visible. Still kinks can make the sag look somewhat disjointed, and this may be used to indicate maximum allowable lengths of straight roads to the sag curve.

KINKS IN PLAN CURVES

In an attempt to find the critical distance from the driver to the curve, the approach distance, 30 perspectives were drawn of curves with radii from 600 to 4000 m and with approach lengths from 100 to 600 m. A portion of one of the series is shown in Figure 4.

When the perspective was observed from the correct viewing distance of 1 m, it became clear that the kink was related to the sharpness of the reversal point. In each series, the perspective with the shortest approach distance to the clearly visible kink was chosen as the critical case. Similarities between the perspectives of critical case were then studied.

As is indicated in Figure 4, the critical case has the angle β (between the two asymptotes) at about 2.5 deg; therefore, when β is larger than 2.5 deg, the curve will be observed as open. The following relationship can thus be established.

$$\tan \beta = \frac{(2h/Z)}{(Z/R_H)} = \frac{2R_H h}{Z^2} \tag{6}$$

or

$$Z^2 = 2R_H h/\tan \beta \tag{7}$$

for $\beta = 2.5$ deg,

$$\tan \beta = 0.044 \tag{8}$$

so that

$$Z^2 = 46R_H h \tag{9}$$

Figure 3. Profile of crest curves on road.

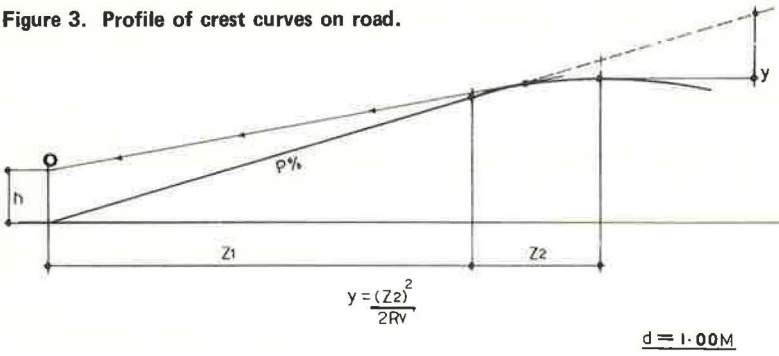

Figure 4. Series of horizontal curves on equal radii from different approach distances.

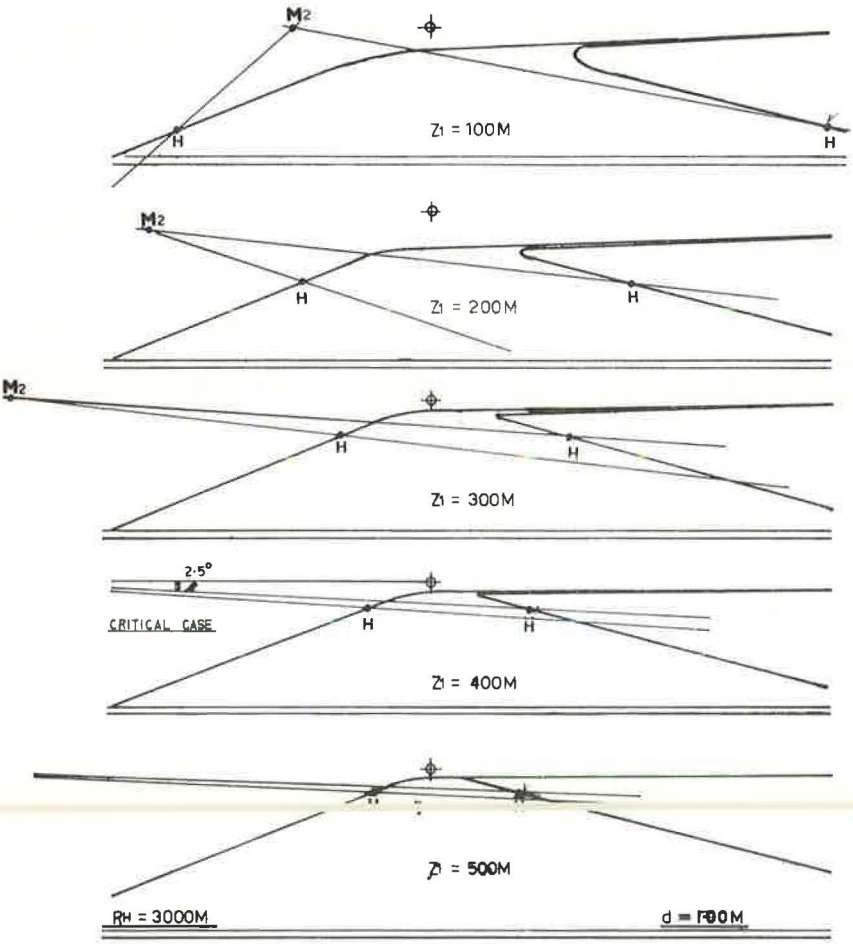

This result is similar to the conclusion drawn from an investigation in the Netherlands; the minor difference lies in the manner of derivation (1). Earlier it was shown that

$$Z^2 = 2R_H a_r + Z_1^2 \quad (1)$$

By substitution, the following general relationship for all horizontal curves can be derived.

$$Z_1^2 = R_H (46h - 2a) \quad (10)$$

where a is the distance from the driver to road edge, to the left for a curve to the left and to the right for a curve to the right.

Equation 10 shows that the maximum approach length to a curve depends on the curve radius and the road width. An approach longer than this maximum will present the curve to the driver as a kink. When approaching nearer than Z_1, the driver will see the curve as open and can adjust his or her driving if necessary. Figure 5 shows curves of different radii and approach lengths where the kinks are similar.

From equation 10 it follows that, the wider the road is, the shorter the critical approach length will be.

CREST CURVES

It was observed earlier that crest curves show no kink. However, it has long been recognized that a driver must see a portion of the crest before he or she gets the feel of the curve (3, 4).

Thirty perspectives were produced of crests with different radii and approach lengths. A portion of one series of these is shown in Figure 6. Similarities were sought between those perspectives that just contained enough information for the driver to read the crest. Again the angle between the two asymptotes was the common factor. At $\alpha = 70$ deg, all crests began to be readable.

From Figure 6,

$$\tan \alpha = \frac{2a_r}{Z_1} \qquad \frac{2hR_v + Z_1^2}{Z_1 R_v} \quad (11)$$

For $\alpha = 70$ deg,

$$Z_1^2 = R_{vc} (0.73a_r - 2h) \quad (12)$$

In this case, the acceptable approach will be longer when the road is wider. I think the driver gets more clues from the road edge on the driver's side.

SAG CURVES

Thirty perspectives were drawn, and the angle between the asymptotes was the common critical factor. The critical angle was measured to be $\alpha = 35$ deg (Figure 7). This leads to

Figure 5. Different plan curves from their critical approach distances.

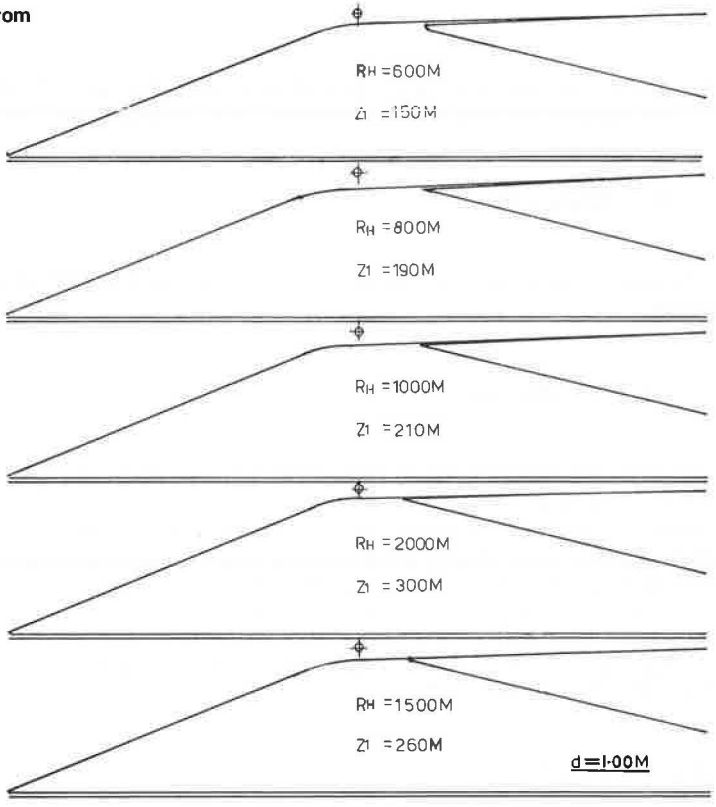

Figure 6. Series of crests of different radii but equal approach distances.

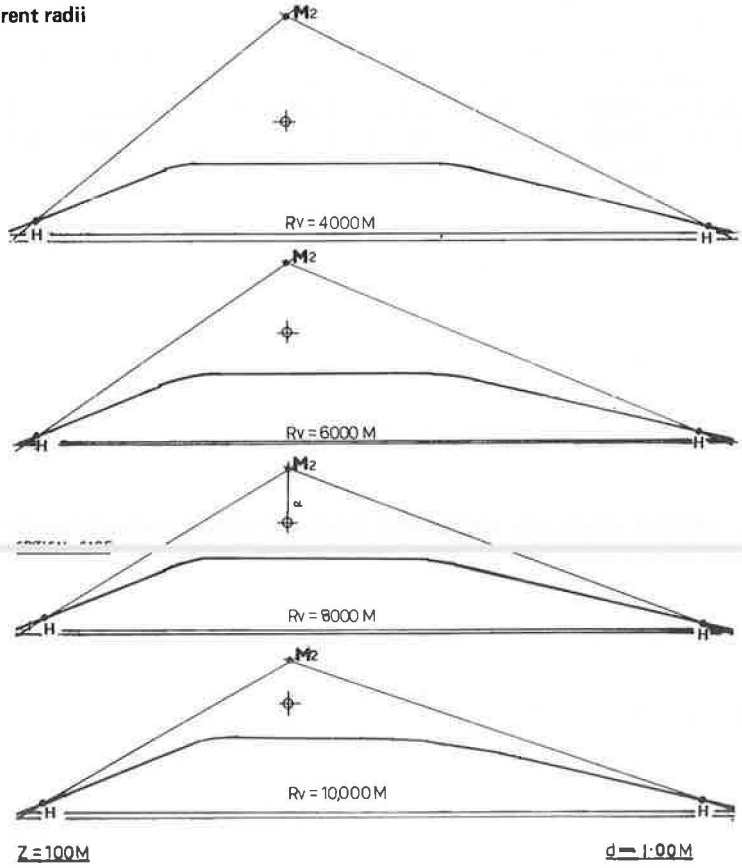

$$Z_1^2 = R_{v_s} (2.6a + 2h) \quad (13)$$

As before, the wider the road is, the longer the acceptable approach will be. In addition, the approach to sag curves can be much longer than the approach to crests when all other conditions are equal.

COMBINED HORIZONTAL AND VERTICAL CURVES

Whenever the plan curve is combined with a crest or a sag curve, whether they are of equal length and in phase or not, there will always be a section of the road that can be seen as a combined curve. This combined curve can be assumed to be a helix for the purpose of this discussion (1).

Therefore, in a long plan curve with a vertical curve somewhere along its length, the section would be analyzed as one part circular plan curve, one part combined curve, and one part circular plan curve.

The simple plan or vertical portions of curves have been discussed previously. The following attempts to analyze the visual consequences of approaches to combined curves.

Crest-Plan Curve

Other authors have already indicated that for crest-plan curves the section of horizontal curve visible to the driver must have at least 2.5 deg deflection (3, 4, 5). At the same time, the maximum approach to the crest must be such that the driver reads its vertical curvature. There is no need to consider the kink in the plan curve because the crest is at the end of the length of visible pavement.

This leads to four equations that must be fulfilled.

$$Z_1^2 = R_{v_c} (0.73a_r - 2h) \quad (12)$$

$$Z_2 = 0.044\, R_H \quad \text{(for a deflection of 2.5 deg)} \quad (14)$$

$$Z = Z_1 + Z_2 \quad (15)$$

$$Z^2 = 2R_v h + Z_1^2 \quad (5)$$

Combination of these equations leads to a relationship that indicates the maximum ratio between R_H and R_v.

$$R_H = \sqrt{R_v}\,(\sqrt{380\ a} - \sqrt{380\ a - 1004\ h}) \quad (16)$$

On a two-lane rural road, where $a_r = 5$ m and $h = 1.2$ m, equation 16 becomes

$$R_H = 17\sqrt{R_v} \quad (17)$$

and

$$Z_1 = 1.11\sqrt{R_v} \quad (18)$$

This relationship between R_H and R_v must be understood in the context of equations 17 and 18.

Provided the plan curve radius is smaller than $17\sqrt{R_v}$, the driver will be able to read the crest at an approach distance of $1.11\sqrt{R_v}$ while the deflection in the visible section of the horizontal curve is larger than 2.5 deg.

Although equation 12 seems excessively complex, design policies would carry, of course, values of R_H with relation to R_v for specific road widths because h is uniform.

Sag-Plan Curve

The full length of the sag-plan curve can be seen from the approach road. A kink, as a result of the plan or of the vertical curve, may be visible and, therefore, needs to be considered.

Only if the approach length is less than the smallest of those permitted for simple plan or vertical curves will no kink be seen by the driver. Therefore,

$$Z_1 \begin{cases} Z_1 = R_H\,(46h - 2a) \\ Z_1 = R_v\,(2.6a + 2h) \end{cases} \tag{19}$$

A critical combination curve is reached when

$$R_H\,(46h - 2a) = R_v\,(2.6a + 2h)$$

or

$$\frac{R_H}{R_v} = \frac{2.6a + 2h}{46h - 2a} \tag{20}$$

Both curves will show a kink when seen from a critical distance. This rather cumbersome equation is simplified for a rural road, where a = 5 m and h = 1.2 m, to

$$\frac{R_H}{R_v} = 0.35 \tag{21}$$

For the ratio to be larger than 0.35, the equation for the vertical curve should be used. When the ratio is smaller than 0.35, the equation for the horizontal curve should be used to calculate maximum length of the approach road.

A somewhat different approach would be to calculate the dominant of the two curves. Combined curves are shown in Figure 8: dominant horizontal in 8a, critical case in 8b, and dominant vertical in 8c. The borderline case between these is found when the combined curve asymptote, $-\infty$, coincides with the extension of the image of the outside edge of the road pavement in the curve (2).

From the figure it can be seen that, if $\tan \alpha < \tan \beta$, the curve is a dominant plan curve, and, if $\tan \alpha > \tan \beta$, the curve is a dominant vertical curve.

In the critical case, $\tan \alpha = \tan \beta$ or

$$\frac{R_H}{R_v} = \frac{h}{a} \tag{22}$$

where a is to outside curbline.

Figure 7. Sag-curve perspective.

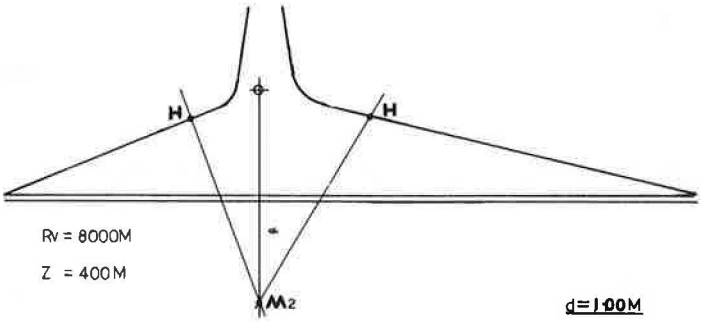

Figure 8. Combined curves: (a) dominant horizontal, (b) critical case, and (c) dominant vertical.

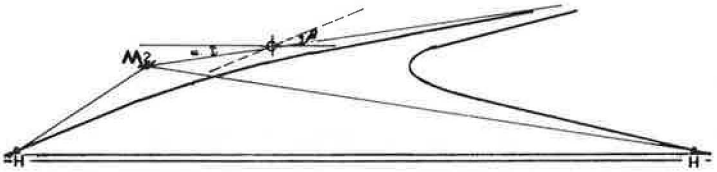

A.

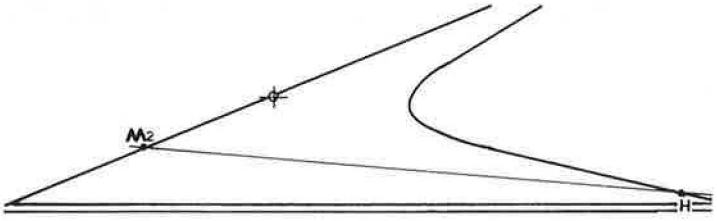

B.

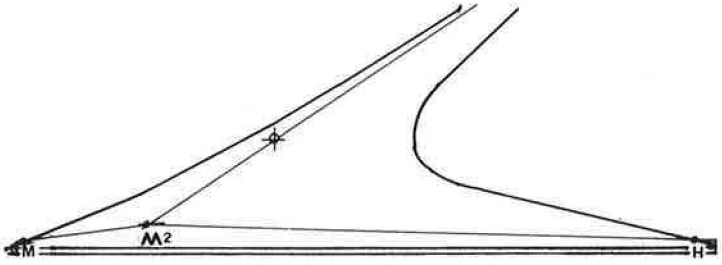

C.

Therefore, when

$$R_H > \frac{h}{a} R_v \tag{23}$$

the combined curve is a dominant-vertical curve, and the approach length must be calculated based on R_v. When

$$R_H < \frac{h}{a} R_v \tag{24}$$

the combined curve is a dominant-plan curve, and the approach length must be calculated based on R_H.

For a rural road with a = 5 m and h = 1.2 m, the critical ratio works out to be 0.24 (2).

REACTION TIME AND KINKS

It is often assumed that the driver reads the road for a distance ahead that is proportional to the speed of the car. Lorenz and Springer (1, 4) suggest that this distance is approximately equal to 10 s of driving time. This agrees with values adopted by me earlier (6). It may not always be the road designer's wish to eliminate all visible kinks in the road alignment. However, it is reasonable to insist that all curves observed from a 10-s distance should be open and readable.

This leads to a relationship between the driver's speed and the road geometry. The 10-s distance is

$$Z_1 = 2.78V \text{ (m)} \tag{25}$$

The critical approach length to the curve in plan is

$$Z_1^2 = R_H (46h - 2a) \tag{7}$$

Substituting and rounding off gives

$$R_H > \frac{V^2}{6h - 0.25a} \tag{26}$$

Similarly, for crest and sag curves respectively, we can derive

$$R_{vc} > \frac{10V^2}{a - 2.5h} \tag{27}$$

$$R_{vs} > \frac{3V^2}{a + 0.75h} \tag{28}$$

The curve radii calculated by equations 27 and 28 are the minimum to be used for a given speed so that an open, nonkink curvature at approach distances equal to up to 10 s of driving can be provided, always provided the curves can actually be seen from these distances.

RESULTS

The results are expressed in a form that would indicate mathematical precision. It should not be overlooked, however, that they are based on some degree of subjective judgment of simplified road perspectives. The outcome of calculations of critical distances should, as a result, be regarded as a guide figure and not as a precise distance. Since this is really all that a designer requires to help in decisions, this limitation on the result is not serious.

Note also that, for a designer to use the results, decisions would have to be made about whether it is necessary to provide alignments without kinks. A critical approach time (such as 10 s) may also be set during which the driver must see the curve as open. If these requirements are to be satisfied, small approach straights will require following curves of much larger radii than the traditional considerations of driver dynamics would prescribe. For a design speed, where V = 100 km/h, a_r = 4.7 m, and h = 1.2 m,

$$R_{H_{open}} > \frac{(100)(100)}{7.20 - 1.25} = 1680 \text{ m} \quad (D_c < 1.04 \text{ deg}) \tag{29}$$

Dynamic considerations would give

$$R_H > \frac{V^2}{127(E+F)} > \frac{10\,000}{127(0.20)} = 393.7 \text{ m} \quad (D_c < 4.44 \text{ deg}) \tag{30}$$

CONCLUSIONS

The following relationships have been derived from the theory developed in the tangent method of perspective drawing of road pavements.

For plan, crest, and sag curves respectively, the maximum approach distances to curves so that they are readable are

$$Z_1^2 = R_H (46h - 2a) \tag{10}$$

$$Z_1^2 = R_{vc} (0.73a_r - 2h) \tag{12}$$

$$Z_1^2 = R_{vs} (2.6a + 2h) \tag{13}$$

For the combined sag-curve plan, the same equation can be used considering that when

$$\frac{R_H}{R_v} > \frac{2.6a + 2h}{46h - 2a} \tag{31}$$

the curve is treated as a vertical curve and when

$$\frac{R_H}{R_V} < \frac{2.6a + 2h}{46h - 2a} \tag{32}$$

the curve is treated as a horizontal curve.

For crest-plan curves,

$$\frac{R_H}{R_V^{1/2}} < (380a)^{1/2} - (380a - 1000h)^{1/2} \tag{33}$$

The curve will be open and give sufficient visual information to the driver for him or her to read the properties of the crest at the critical distance for the crest.

So that drivers are given a timely indication of the properties of the curve, head alignment radii should be chosen so that, for plan, crest, and sag curves respectively,

$$R_H > \frac{V^2}{6h - 0.25a} \tag{26}$$

$$R_{VC} > \frac{10\ V^2}{a - 2.5h} \tag{27}$$

and

$$R_{VS} > \frac{3V2}{a + 0.75h} \tag{28}$$

ACKNOWLEDGMENT

I would like to thank Springer and Huizinga for the patience and helpful guidance they provided while I was at the Bureau of Road Aesthetics of Rijkswaterstaat in Utrecht, Netherlands, during 1973.

REFERENCES

1. J. F. Springer and K. E. Huizinga. The Road Perspective as a Test of the Road Design. Rijkswaterstaat, Netherlands.
2. J. F. Springer, K. E. Huizinga, and A. M. Moonen. Thoughts on Aesthetically Acceptable Roadforms. WEGEN, May 1970—.
3. Guidelines for Road Design, Part 2: Raumliche Linienführung. Forschungsgesellschaft für das Strassenwesen, 1970.
4. E. H. H. Lorenz. Alignment and Form of Roads and Expressways. Bauverlag GmbH, Wiesbaden and Berlin.
5. C. Tunnard and B. Pushkarev. Man Made America. Yale Univ. Press.
6. T. ten Brummelaar. Simple Panoramic Perspectives. Journal, Australian Road Research Board, Vol. 4, No. 9, June 1972.

APPENDIX

DERIVATIONS

The derivation of equation 1 in which the distance from the driver to a reversal point is determined follows. From Figure 1, x on the plan view is shown as D on the perspective.

From the plan view,

$$x \approx a_r + \frac{Z_2^2}{2R_H} \tag{34}$$

and

$$Z_2 = Z - Z_1 \tag{35}$$

where Z_1 is a constant.

From the perspective view,

$$D = \frac{x}{Z} = \frac{a_r + \frac{Z_2^2}{2R_H}}{Z} = \frac{2R_H a_r + (Z - Z_1)^2}{2R_H Z} \tag{36}$$

At the reserval point, D will have a minimum length, or

$$\frac{dD}{dZ} = 0 \tag{37}$$

This differentiation leads to

$$Z^2 = 2R_H a_r + Z_1^2 \tag{1}$$

The analysis of equation 5 in which the distance from the driver to the visible top of a crest is determined follows. From Figure 3, the form of the crest is

$$\text{Crest form} = PZ_2 - \frac{Z_2^2}{2R_v} \tag{38}$$

The slope of the tangent to the crest is

$$\text{Tangent slope} = P - \frac{Z_2}{R_v} \tag{39}$$

The slope of a light ray from the crest to the driver is

$$\text{Light-ray slope} = \frac{ZP - \left(\frac{Z_2^2}{2R_v}\right) - h}{Z} \tag{40}$$

and must be equal to the slope of the tangent. Therefore,

$$\frac{ZP - \left(\frac{Z_2^2}{2R_v}\right) - h}{Z} = P - \frac{Z_2}{R_v} \tag{41}$$

where

$$Z_2 = Z - Z_1 \tag{42}$$

This leads to

$$Z^2 = 2R_v h + Z_1^2 \tag{5}$$

SPONSORSHIP OF THIS RECORD

GROUP 2—DESIGN AND CONSTRUCTION OF TRANSPORTATION FACILITIES
W. B. Drake, Kentucky Department of Transportation, chairman

GENERAL DESIGN SECTION
F. W. Thorstenson, Minnesota Department of Highways, chairman

Committee on Geometric Design
B. H. Rottinghaus, Howard, Needles, Tammen and Bergendoff, chairman
Alvin R. Cowan, Federal Highway Administration, secretary
James D. Anderson, P. B. Coldiron, Harold D. Cooner, W. M. Foster, John C. Glennon, Malcolm D. Graham, C. W. Gray, William R. Hawkins, Peter J. Hunt, Frank J. Koepke, Jack E. Leisch, John Robert Moore, Geoffrey M. Nairn, Jr., George B. Pilkington II, Stanley L. Ring, M. D. Shelby, Bob L. Smith, Robert A. Snowber, John B. Wilkes, W. A. Wilson

Committee on Hydrology, Hydraulics, and Water Quality
Samuel V. Fox, Texas Highway Department, chairman
Frank L. Johnson, Federal Highway Administration, secretary
Alvin G. Anderson, John J. Bailey, Jr., Harry H. Barnes, Jr., Mike Bealey, Lawrence D. Bruesch, Earl C. Cochran, Jr., Allen L. Cox, Richey S. Dickson, Kenneth S. Eff, Gene R. Fiala, Philip F. Frandina, John L. Grace, Jr., Lester A. Herr, N. J. McMillen, William O. Ree, Brian M. Reich, John E. Sandahl, William P. Somers, Adrianus Van Kampen, A. Mainard Wacker

Committee on Subsurface Structures Design
John G. Hendrickson, Jr., Greeley and Hansen, chairman
Roger L. Brockenbrough, Robert M. Clementson, Richey S. Dickson, Paul D. Doubt, W. B. Drake, Kenneth S. Eff, Kenneth F. Gerleman, Paul M. Heffern, Donald G. Meacham, F. Dwayne Nielson, Eric F. Nordlin, Richard A. Parmelee, M. G. Spangler, R. S. Standley, Harold V. Swanson, David C. Thomas, James D. Washington, R. K. Watkins

Lawrence F. Spaine, Transportation Research Board staff

Sponsorship is indicated by a footnote on the first page of each report. The organizational units and the chairmen and members are as of December 31, 1974.